

TRANSOCEANIC PROPAGATION OF SUMATRA TSUNAMIS AND
THEIR EFFECTS ON MALDIVES ISLANDS

A THESIS SUBMITTED TO
THE GRADUATE SCHOOL OF NATURAL AND APPLIED
SCIENCES
OF
MIDDLE EAST TECHNICAL UNIVERSITY

BY

HAKAN KOYUNCU

IN PARTIAL FULLFILLMENT OF THE REQUIREMENTS
FOR
THE DEGREE OF MASTER OF SCIENCE
IN
CIVIL ENGINEERING

DECEMBER 2010

Approval of the thesis:

**TRANSOCEANIC PROPAGATION OF SUMATRA TSUNAMIS
AND THEIR EFFECTS ON MALDIVES ISLANDS**

submitted by **HAKAN KOYUNCU** in partial fulfillment of the requirements for the degree of **Master of Science in Civil Engineering Department, Middle East Technical University** by,

Prof. Dr. Canan Özgen

Dean, Graduate School of **Natural and Applied Sciences**

Prof. Dr. Güney Özcebe

Head of Department, **Civil Engineering**

Prof. Dr. Ahmet Cevdet Yalçiner

Supervisor, **Civil Engineering Dept., METU**

Examining Committee Members:

Prof. Dr. Ayşen Ergin

Civil Engineering Dept., METU

Prof. Dr. Ahmet Cevdet Yalçiner

Civil Engineering Dept., METU

Doç. Dr. Utku Kanoğlu

Civil Engineering Dept., METU

Dr. Işıkhan Güler

Civil Engineering Dept., METU

Engin Bilyay

General Directory of Railways, Ports and Airports

Date:

09.12.2010

I hereby declare that all information in this document has been obtained and presented in accordance with academic rules and ethical conduct. I also declare that, as required by these rules and conduct, I have cited all material and results that are not original to this work.

Name, Last name : HAKAN KOYUNCU

Signature :

ABSTRACT

TRANSOCEANIC PROPAGATION OF SUMATRA TSUNAMIS AND THEIR EFFECTS ON MALDIVES ISLANDS

Koyuncu, Hakan

MS., Department of Civil Engineering

Supervisor: Prof. Dr. Ahmet Cevdet Yalçiner

December 2010, 64 pages

In recent years the negative effects of tsunamis in the Indian Ocean dramatically increased. Although, this subject became very popular lately, the far-field activities of tsunamis are needed to be evaluated in Indian Ocean. In this thesis, Maldives and Sumatra islands were emphasized to analyze the effects of the transoceanic propagation of tsunamis in Indian Ocean. At first, using GIS Based softwares, the geographical data of the region were extracted and organized for analyzing. Secondly, a worst earthquake scenario was initiated at Sumatra which is located at a long distance from Maldives Islands. Then, corresponding effects of transoceanic tsunami were analyzed and accordingly coastal amplifications near Maldivian Islands were computed by NAMI DANCE. As a final step, an evaluation study was carried out to understand the transoceanic propagation behavior of tsunamis in Indian Ocean and results were discussed.

Keywords: Tsunami, Transoceanic, Maldives Islands, Sumatra.

ÖZ

SUMATRA KAYNAKLI TSUNAMİLERİN UZAK ALAN İLERLEMESİ VE MALDİV ADALARINA ETKİSİ

Koyuncu, Hakan

Yüksek Lisans, İnşaat Mühendisliği Bölümü

Tez Yöneticisi: Prof. Dr. Ahmet Cevdet Yalçın

Aralık 2010, 64 sayfa

Geçtiğimiz yıllarda tsunamilerin Hint Okyanusundaki olumsuz etkileri hissedilebilir derecede artmıştır. Bu konunun son zamanlarda yaygın olarak araştırılmaya başlanmasına rağmen, Hint Okyanusu'nda gerçekleşebilecek olan olası tsunamilerin uzak alan ilerlemelerinin değerlendirilip yorumlanması gerekmektedir. Bu tezde, Maldivler ve Sumatra adaları ele alınarak, Hint Okyanusunda ortaya çıkabilecek olan olası bir tsunaminin uzak alan ilerlemesi analiz edilmeye çalışılmıştır. İlk aşamada, coğrafi bilgi sistemlerinden faydalanılarak hazırlanan bilgisayar programları kullanılmış ve incelenecek olan bölgenin hem deniz taban topoğrafyası hem de kıyı alanı kara topoğrafyasına ait sayısal veriler elde edilip, düzenlenmiştir. İkinci aşamada, deprem seneryoları arasından Maldiv adaları için en çok tehlike yaratabilecek olanlar seçilmiş ve tsunami hareketleri modellenmiştir. Buna bağlı olarak, tsunami dalgalarının uzak alan ilerlemeleri analiz edilmiş, Maldiv adaları etrafında görülmesi muhtemel olan dalga yükseklikleri NAMI DANCE programı ile bulunmuştur. Son olarak, bulunan sonuçlar değerlendirilmiş ve Hint Okyanusun da oluşabilecek olan tsunamilerin uzak alan ilerlemelerinin daha iyi anlaşılmasında kullanılmıştır.

Anahtar kelimeler: Tsunami, Uzak Alan, Maldiv Adaları, Sumatra.

ACKNOWLEDGMENTS

I would like to express my sincere appreciation to Prof. Dr. Ahmet Cevdet Yalçiner not only for his great knowledge and experiences he shared but also for his understanding, patience and encouragement throughout my Ms. study. I would like to thank to Prof. Dr. Ayşen Ergin and Dr. Işıkhan Güler for enlightening me with their great knowledge in coastal engineering.

I would also like to thank to Ms. Ceren Özer for not only her valuable discussions and recommendations in my study but also her friendship and supports.

Special thanks to the staff of the Coastal Engineering Research Center, especially to Ms. Hülya Karakuş, Mr. Cüneyt Baykal and Mr. Mustafa Esen for encouraging me through my study.

The endless motivation, encouragements and patience of Ms. Seçil Özdemir makes everything more amusing and easy throughout this study.

I also want to thank to my dear friend Ms. Özben Örs for her friendly and kind aids together with her endless motivation.

Finally, the presence of such a precious family makes everything less complicated. I want to express my thanksgiving to them for their endless love and encouragement.

TABLE OF CONTENTS

PLAGIARISM	iii
ABSTRACT	iv
ÖZ	v
ACKNOWLEDGMENTS	vi
TABLE OF CONTENTS	vii
LIST OF FIGURES	viii
LIST OF TABLES	x
CHAPTERS	
1.INTRODUCTION	1
2.LITERATURE SURVEY	6
3.NUMERICAL BACKGROUND and TSUNAMI SOURCE SELECTION	14
3.1.Numerical Background	14
3.2.Bathymetry Processing	16
3.3.Correlation Studies	17
3.4.Tsunami Source Selection	20
3.5.Selection of Gauges	25
4.SUMMARY OF MODELING STUDIES	28
4.1.Domain Selection	28
4.2.Propagation of Tsunamis	30
4.2.1.Sumatra-Andaman Earthquake, 2004	31
4.2.2.Megathrust under the Batu and Mentawai Islands (McCloskey et al., 2007)	40
4.2.3.Megathrust under the Batu and Mentawai Islands (Okal and Synolakis., 2007)	46
4.3.Summary	49
5.DISCUSSION AND CONCLUSION	61
5.1.General Evaluation	61
5.2.Discussions and Conclusions	62
5.2.Suggestions for Further Studies	63
REFERENCES	65

LIST OF FIGURES

FIGURES

Figure 1 :	The numerical modeling simulation of waveform of the tsunami that must have been experienced at Male after December 2004 earthquake (Harinarayana and Hirata, 2005).	8
Figure 2 :	Spherical projection of the project area taken from Google Earth.	18
Figure 3 :	Planar projection of the project area transformed from spherical projection of Google Earth by AutoCAD Raster Design.	19
Figure 4 :	Initial water surface elevation for the Sumatra-Andaman earthquake, 2004	21
Figure 5 :	Initial water surface elevation for the second case. (McCloskey et al., 2007)	22
Figure 6 :	Map of tsunamigenic earthquake scenarios. (Okal and Synolakis, 2007)	23
Figure 7 :	Initial water surface elevation for the third case. (Okal and Synolakis, 2007)	25
Figure 8 :	Location and distribution of selected gauge points.	27
Figure 9 :	Demonstration of selected domains for nested analysis.	29
Figure 10 :	Gauges located at Maldives Islands in Domain C and E.	30
Figure 11 :	Arrival time of first wave for Sumatra-Andaman earthquake, 2004.	31
Figure 12 :	Arrival time of the maximum wave for Sumatra-Andaman earthquake, 2004.	32
Figure 13 :	Sea states between t=0 and t=420 min. for Sumatra-Andaman earthquake, 2004.	33
Figure 14 :	Sea states between t=480 and t=540 min. for Sumatra-Andaman earthquake, 2004.	34
Figure 15 :	Maximum positive and negative wave amplitudes in Domain C for Sumatra-Andaman Earthquake, 2004.	35
Figure 16 :	Maximum positive and negative wave amplitudes in Domain E for Sumatra-Andaman Earthquake, 2004.	36
Figure 17 :	Tide gauges record in Hanimaadoo, Male and Gan islands during 26th December 2004 Sumatra-Andaman earthquake. (Based on NOAA, USA)	39
Figure 18 :	Arrival time of first wave for the 2 nd case. (McCloskey et al., 2007)	40
Figure 19 :	Arrival time of the maximum wave for the 2 nd case. (McCloskey et al., 2007)	41
Figure 20 :	Sea states between t=0 and t=300 min for the 2 nd case (McCloskey et al., 2007)	42

Figure 21 :	Sea states between t=360 and t=540 min. for the 2 nd case (McCloskey et al., 2007)	43
Figure 22 :	Maximum positive and negative wave amplitudes in Domain C for the 2 nd case. (McCloskey et al., 2007)	44
Figure 23 :	Maximum positive and negative wave amplitudes in Domain E for the 2 nd case. (McCloskey et al., 2007)	45
Figure 24 :	Maximum positive and negative wave amplitudes in Domain C for the 3 rd case. (Okal and Synolakis, 2007)	47
Figure 25 :	Maximum positive and negative wave amplitudes in Domain E for the 3 rd case. (Okal and Synolakis, 2007)	48
Figure 26 :	Time history of water surface fluctuations for selected gauges in Domain C.	53
Figure 27 :	Time history of water surface fluctuations for selected gauges in Domain E.	57
Figure 28 :	Cross-Section of the line between Sumatra and Maldives Islands and time history graphs of water level fluctuations at some points.	60

LIST OF TABLES

TABLES

Table 1 :	Details of the earthquake activity of major events [>6] near the Sumatra between 2004 and 2010 (USGS).	7
Table 2 :	Rupture characteristics of the Sumatra-Andaman earthquake, 2004, (Lay et al., 2005)	20
Table 3 :	Rupture characteristics of the earthquake selected as the second case. (McCloskey et al., 2007)	22
Table 4 :	Rupture characteristics of the earthquake selected as the third case. (Okal and Synolakis, 2007)	24
Table 5 :	Coordinates of selected gauge points.	25
Table 6 :	Boundary coordinates of domains.	29
Table 7 :	Results of simulation study in Domain C for Sumatra-Andaman earthquake, 2004.	36
Table 8 :	Results of simulation study in Domain E for Sumatra-Andaman earthquake, 2004.	37
Table 9 :	Tide gauge observations (Merrifield et al., 2005) and computed maximum positive wave amplitudes.	39
Table 10 :	Results of simulation study in Domain C for the 2 nd case. (McCloskey et al., 2007)	45
Table 11 :	Results of simulation study in Domain E for the 2 nd case. (McCloskey et al., 2007)	46
Table 12 :	Results of simulation study in Domain C for the 3 rd case. (Okal and Synolakis, 2007)	48
Table 13 :	Results of simulation study in Domain E for the 3 rd case. (Okal and Synolakis, 2007)	49
Table 14 :	Summary of simulation studies for all cases in Domain C.	58
Table 15 :	Summary of simulation studies for all cases in Domain E.	59

CHAPTER I

INTRODUCTION

The coastal zone makes up only 4% of the world's land area but is home to one-third of the world's population, a proportion that is predicted to double over the next 15 years. Coastal zones are important since they generally contain a wide range of ecosystems which are economically significant and rich in biological resources, such as coral reefs, seagrass beds, lagoon, etc. The projected population growth and rapid development in coastal regions consequently makes the ecosystems and human settlements in these regions become more vulnerable to natural hazards (UNEP-WCMC, 2006).

Tsunami resulting from massive and rapid displacement, affects not only the area where it is generated, but also the substantial distance away from the epicenter. The term tsunami comes from the Japanese language meaning harbor wave, can be defined as a complex oscillating seismic sea wave generated due to large scale disturbance of land under the sea in a relatively short time duration. As tsunami cases be more evident in near history of world and experienced with the immense effects on damage to life and property, tsunamis are accepted to be the most hazardous disaster the among coastal area disasters (Harinarayana and Hirata, 2005).

Technically, according to Harinarayana and Hirata (2005), tsunamis are generated mainly due to sudden displacement of the sea bottom surface that generates near vertical disruption of the water column. Vertical disruptions such as the onset of earthquakes under the sea are more frequent when it comes to occurrences. Volcanic eruptions, displacement of marine sediments, landslides near the coast, man-made nuclear explosions in the sea and meteor impact from space can also generate destructive tsunamis.

Differently, tsunamis can also be categorized according to their location of generation. If the source is within the 1000 km of the shoreline, tsunami is called as near-field or near-shore. On the contrary, if tsunami source lies outside the 1000 km zone from the shoreline, then it's called as far-field or transoceanic tsunami. However, it should not be noted that the distance from the shoreline is something relative as one tsunami can be called as a far-field type with respect to one shore, and near-field type with respect to another (Sümer et al., 2007).

Generation of a tsunami is another complex phenomena which draws researchers attention to the threat of inundation in coastal zones. Looking deeply over the nature of tsunamis, considerable amount of researches on this subject are mainly concentrated on two tsunami-making incidents; fault break and landslides, which have different features.

Okal and Synolakis (2004) state that Tsunamis generated by submarine landslides have comparatively large run-up height, but have more limited far-field effects than earthquake tsunamis. According to the authors, the most likely explanation for this is that the energy available for the tsunami is proportional to the square of the seabed uplift. Therefore, a submarine landslide that move less

material, is said to be able to move it vertically up to 100 times as much as an earthquake resulting in a comparable amount of tsunami energy can (Okal and Synolakis, 2004).

Okal and Synolakis (2004), in the same study points out that, the wave generation is subjective to the depth at which submarine landslides and earthquakes occur. As illustrated by Ward (2001), for a landslide occurring in shallow water, effects of critical landslide motion give large localized waves, resulting in more hazardous waves than the landslide cases occurring in deep water.

On the other hand, Okal and Synolakis (2004), agreeing with Harbitz et al. (2006), claim that, tsunamis generated by earthquakes are surprisingly more hazardous when the seabed displacement occurs in deeper waters. As the initial wave will become shorter and higher as a result of shoaling propagating from deeper to shallower waters, the effects are more severe on coastal regions.

As explained above; generation of tsunamis is a complex phenomena. The researchers investigating the inundation in coastal zones exemplified the effectants of tsunami and the cases with their levels of effect and severity.

Vigny and many other researchers point out the great magnitude 9.2 Sumatra–Andaman earthquake of 26 December 2004 resulted from up to 20 m of slip on the Sunda megathrust which, in turn, produced vertical seafloor displacements. These vertical movements, approaching 5 m in the deep water above the Sunda trench southwest of the Nicobar Islands and off-shore Aceh created a large tsunami that propagated throughout the Indian Ocean, killing more than 250,000 people. (Vigny et al., 2005; Subarya et al., 2006; Piatanesi and Lorito, 2007; Chlieh et al., 2007)

As the megathrust ruptured again in the magnitude 8.7 Simeulue–Nias earthquake occurred on March 28 2005. While locally the slip on the megathrust was as high as 12 m (Briggs et al., 2006) the resulting tsunamis were below the height of 4 m (Geist et al., 2005) and the smaller death toll was largely due to strong ground shaking. As McCloskey et al. (2007) stresses, the contrast was only partly due to the smaller energy release of the second earthquake.

Following, as McCloskey et al (2007) stated; the greatest slip in December 2004 produced large vertical seafloor displacements under deep water, resulting in a tsunami with high potential energy and (Leblond and Mysak, 1978), large wave amplification toward the coast. As McCloskey points the contrary out, in the March 2005, the maximum slip event created seafloor movements in relatively shallow water, which resulted in a tsunami with lower wave amplification and smaller potential energy.

By McCloskey, it is claimed to be clear that the contrasting tsunamis produced by these earthquakes was the result of complex interactions between their moment release, distributions of slip and the local and regional bathymetry. (McCloskey et al, 2007)

After all, the massive Sumatra–Andaman earthquake of 9.2 magnitude earthquake severely affected the lives of millions of people (California Institute of Technology, 2008). With no ocean based sensor system deployed in the Indian Ocean, it is accepted to become the worst natural disaster in history as a result of a tsunami caused by an earthquake. (Blewitt et al., 2006) Megawati and Pan (2009) investigating seismic hazard and risk levels caused by the potential giant earthquakes at major cities; some of which are in Sumatra, believes several lines indicating that the Mentawai segment of the

Sumatran megathrust is very likely to rupture within the next few decades.

Given this background, in this study, transoceanic propagation of tsunamis in Indian Ocean was investigated by focusing on the Sumatra and Maldives Islands principally. For the worst case scenarios and case studies tsunami modeling study was applied to the specified locations, using different rupture-specific tsunami sources which can generate tsunamis. In chapter 1, an introduction which included brief information about tsunamis and active seismic zone in Sumatra was given. The literature survey carried out for this thesis was given in Chapter 2. In literature survey part, previous studies on the thesis subject and different approaches of researches were given. In Chapter 3, numerical background and tsunami source selection study were defined. In chapter 4, brief summary of modeling study was represented and illustrated with figures. As a final, an evaluation of the study and suggestions for further studies were given in Chapter 5.

CHAPTER II

LITERATURE SURVEY

Although the frequency of catastrophic events seems to be large, they occur in time in non-uniformly way. To reduce the detrimental effects of these events, necessary analysis and observations should be done based on the scientific knowledge.

The uniqueness of 2004 earthquake and consequent tsunami in Indian Ocean cannot be an excuse to justify the loss of lives and property which may have decreased by the necessary precautionary measures and mitigation strategies. The 26 December 2004 earthquake was occurred in a well-known zone of weakness in the Earth's crust, extending from near the Andaman Islands in the Indian Ocean along the islands of Sumatra, Java, Bali, Lombok, etc., through to New Guinea and beyond. This weak tectonic zone, which has been subjected to geological studies, is characterized by frequent earthquakes and a very large number of active volcanoes. Earthquakes, which had a magnitude greater than 6 and occurred in between 2004 and 2010 is given in a tabulated form in Table 1.

Table 1. Details of the earthquake activity of major events (>6) near the Sumatra between 2004 and 2010 (USGS).

Year	Month	Day	Lat.	Longt.	Depth	Magn.	Year	Month	Day	Lat.	Longt.	Depth	Magn.
2004	2	22	-1.56	100.49	42.00	6.00	2006	7	17	-9.42	108.32	21.00	6.10
2004	4	16	-5.21	102.72	44.00	6.00	2006	7	19	-6.53	105.39	45.00	6.10
2004	5	11	0.41	97.82	21.00	6.10	2006	7	27	1.71	97.15	20.00	6.30
2004	7	25	-2.43	103.98	582.00	7.30	2006	8	11	2.40	96.35	22.00	6.20
2004	12	26	3.30	95.98	30.00	9.10	2006	12	1	3.39	99.08	204.00	6.30
2004	12	26	6.34	93.36	30.00	6.10	2006	12	22	10.65	92.36	24.00	6.20
2004	12	26	7.42	93.99	30.00	6.00	2007	1	8	8.08	92.44	11.00	6.10
2004	12	26	5.50	94.21	30.00	6.10	2007	3	6	-0.49	100.50	19.00	6.40
2004	12	26	6.85	94.67	30.00	6.00	2007	3	6	-0.49	100.53	11.00	6.30
2004	12	26	6.91	92.96	39.00	7.20	2007	4	7	2.92	95.70	30.00	6.10
2004	12	26	8.88	92.38	16.00	6.60	2007	6	26	-10.49	108.15	10.00	6.00
2004	12	26	13.46	92.74	26.00	6.30	2007	7	25	7.16	92.52	15.00	6.10
2004	12	26	13.53	92.84	13.00	6.20	2007	8	8	-5.93	107.68	291.00	6.10
2004	12	26	3.65	94.09	17.00	6.00	2007	8	8	-5.86	107.42	280.00	7.50
2004	12	26	2.79	94.16	30.00	6.10	2007	9	12	-4.44	101.37	34.00	8.50
2004	12	27	5.35	94.65	35.00	6.10	2007	9	12	-2.62	100.84	35.00	7.90
2004	12	29	9.11	93.76	8.00	6.10	2007	9	13	-1.69	99.67	28.00	6.50
2004	12	29	8.79	93.20	12.00	6.20	2007	9	13	-2.13	99.63	22.00	7.00
2004	12	31	7.12	92.53	14.00	6.10	2007	9	13	-3.17	101.52	53.00	6.00
2004	12	31	6.20	92.91	11.00	6.00	2007	9	14	-4.07	101.17	23.00	6.40
2005	1	1	5.10	92.30	11.00	6.70	2007	9	19	-2.75	100.89	35.00	6.00
2005	1	1	7.34	94.46	55.00	6.10	2007	9	20	-2.00	100.14	30.00	6.70
2005	1	2	6.36	92.79	30.00	6.40	2007	9	26	-1.79	99.49	26.00	6.10
2005	1	4	10.67	92.36	23.00	6.10	2007	9	29	2.90	95.52	35.00	6.00
2005	1	9	4.93	95.11	40.00	6.10	2007	10	4	2.54	92.90	35.00	6.20
2005	1	15	-6.46	105.24	58.00	6.00	2007	10	24	-3.90	101.02	21.00	6.80
2005	1	24	7.33	92.48	30.00	6.30	2007	11	25	-2.24	100.41	35.00	6.00
2005	1	26	2.70	94.60	22.00	6.20	2007	12	22	2.09	96.81	23.00	6.10
2005	2	5	2.26	94.99	30.00	6.00	2008	1	4	-2.78	101.03	35.00	6.00
2005	2	9	4.80	95.12	44.00	6.00	2008	1	22	1.01	97.44	20.00	6.20
2005	2	26	2.91	95.59	36.00	6.80	2008	2	20	2.77	95.96	26.00	7.40
2005	3	28	2.09	97.11	30.00	8.60	2008	2	24	-2.40	99.93	22.00	6.50
2005	3	28	0.92	97.87	36.00	6.10	2008	2	25	-2.49	99.97	25.00	7.20
2005	3	30	2.99	95.41	22.00	6.30	2008	2	25	-2.33	99.89	25.00	6.60
2005	4	3	0.37	98.32	30.00	6.00	2008	2	25	-2.24	99.81	25.00	6.70
2005	4	3	2.02	97.94	36.00	6.30	2008	3	3	-2.18	99.82	25.00	6.20
2005	4	8	-0.22	97.73	20.00	6.10	2008	3	15	2.71	94.60	25.00	6.00
2005	4	10	-1.64	99.61	19.00	6.70	2008	3	29	2.86	95.30	20.00	6.30
2005	4	10	-1.71	99.78	30.00	6.50	2008	5	19	1.64	99.15	10.00	6.00
2005	4	10	-1.59	99.72	30.00	6.40	2008	6	27	11.01	91.82	17.00	6.60
2005	4	11	2.17	96.76	24.00	6.10	2008	6	28	10.85	91.71	15.00	6.10
2005	4	16	1.81	97.66	31.00	6.40	2008	8	10	11.06	91.81	20.00	6.20
2005	4	28	2.13	96.80	22.00	6.20	2008	11	22	-4.35	101.26	24.00	6.30
2005	5	10	-6.23	103.14	17.00	6.30	2009	4	15	-3.12	100.47	22.00	6.30
2005	5	14	0.59	98.46	34.00	6.70	2009	8	10	14.10	92.89	4.00	7.50
2005	5	18	5.44	93.36	2.00	6.10	2009	8	16	-1.48	99.49	20.00	6.70
2005	5	19	1.99	97.04	30.00	6.90	2009	9	2	-7.78	107.30	46.00	7.00
2005	6	8	2.17	96.72	23.00	6.10	2009	9	30	-0.72	99.87	81.00	7.50
2005	7	5	1.82	97.08	21.00	6.70	2009	10	1	-2.52	101.50	9.00	6.60
2005	7	24	7.92	92.19	16.00	7.20	2009	10	16	-6.53	105.22	38.00	6.10
2005	11	19	2.16	96.79	21.00	6.50	2009	11	10	8.08	91.90	23.00	6.00
2006	2	3	11.86	92.37	19.00	6.10	2009	12	9	2.77	95.91	19.00	6.00
2006	4	19	2.64	93.23	17.00	6.20	2009	12	23	-1.43	99.39	19.00	6.00
2006	4	25	1.99	97.00	21.00	6.30	2010	03	30	13.67	92.83	34.00	6.70
2006	5	16	0.09	97.05	12.00	6.80	2010	04	06	2.38	97.05	31.00	7.80
2006	6	21	6.94	92.45	16.00	6.00	2010	05	09	3.75	96.02	38.00	7.20
2006	6	27	6.50	92.79	28.00	6.30	2010	05	31	11.13	93.47	112.00	6.50
2006	7	17	-9.28	107.42	20.00	7.70	2010	06	12	7.88	91.94	35.00	7.50
2006	7	17	-9.09	107.76	10.00	6.00	2010	10	25	3.49	100.09	20.00	7.80

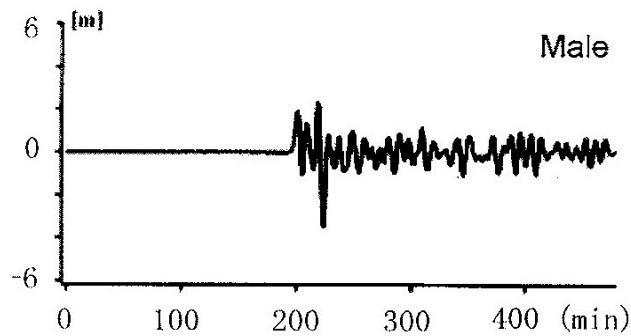


Figure 1. The numerical modeling simulation of waveform of the tsunami that must have been experienced at Male after December 2004 earthquake (Harinarayana and Hirata, 2005).

After 2004, through a study carried out by DCRC group of Tohoku University, available bathymetry data in Indian Ocean was taken as basis and a numerical modeling has been performed. Based on the numerical modeling studies, the initial expected height of the tsunami has been found out to be about 2 to 3 m, with an maximum height of 4 m. The shape of the waveform has been estimated near the earthquake location and this appears to assume a crescent shape almost parallel to the Sunda Trench structure. By Harinanayana and Hirata (2005), the initial wavelength being more than 100 km is said to require 2 to 3 hours, for the initial wave to reach the countries distant such as Sri Lanka and India and 8 to 9 hours to reach the farther countries like Somalia. As a result the modeling studies, high frequency waves were observed near Male as the expected waveform after such a tsunami for that particular region can be seen in Figure 1 (Harinarayana and Hirata, 2005).

Another tsunami threat case in Indian Ocean was also investigated by modeling about 1000 possible complex earthquake ruptures. McCloskey et al., (2007) calculated the seafloor displacements and tsunami height distributions. The most likely 100 scenarios were

used as the initial condition for numerical simulations of tsunami generation and propagation (McCloskey et al., 2007). However, the concentration in particular was on the distribution of wave heights that might be experienced in western Sumatra where the negative effects of near-field tsunamis would be observed.

In this thesis, the focus of attention is partially and locally on Maldives, where hasn't been explored in detail with fine bathymetrical data. The assumptions made are mainly referenced from two studies, one of which is McCloskey's serious study named "Tsunami Threat in the Indian Ocean from a Future Megathrust Earthquake west of Sumatra"; and the other called Okal and Synolakis's article of "Far Field Tsunami Hazard from Megathrust Earthquakes in the Indian Ocean".

In order to be consistent and parallel with previous research findings, here, by referring to McCloskey et al. (2007) and Okal and Synolakis (2007), the subsequent assumptions are made:

- the southern termination of the 1797 event and both the northern and southern terminations of the 1833 event were sourced by barriers to rupture propagation,
 - while any future Mentawai Islands earthquake may rupture any of these barriers, its southern extent will likely be defined by one of them,
 - earthquake rupture will not proliferate beyond the Sunda Strait.

The four rupture lengths considered by the same authors are as follows.

1. Rupture of the 200-km long patch of the megathrust, from the Batu Islands to the north of Sipura that failed in 1797 but not in 1833.

2. Repeat of the 1797 earthquake rupture, between the Batu and south of the Pagai Islands with a total length of about 330 km.

3. Rupture of the 630-km long patch that includes the 1797 and 1833 ruptures and extends south to Enganno Island.

4. A worst case 800-km long rupture scenario extending from beneath Siberut Island through the poorly understood Enganno region to the Sunda Strait.

It is agreed that, while other rupture scenarios are certainly possible, in these scenarios segments are likely to cover a sufficient range of earthquakes. The fourth case; pointed out to be the the ‘worst case’; 800 km long rupture along the Siberut Islands to Engano by McCloskey et al. (2007), is worth studying in the frame of Maldives as there hasn’t been a detailed study in that region.

Moreover, McCloskey et al. (2007) et al agrees that, the systematic study of tsunamis generated from large number of earthquakes simulated using complex slip distributions and sophisticated elastic displacement models, as spread of a well- constrained bathymetric model, offers an opportunity to present the boundary conditions for a tsunami model simulating wave. Therefore, an estimate of the tsunami threat posed by the next great Mentawai earthquake is made and systematic relationships between the earthquake source and the predicted tsunami amplitudes are examined throughout the following parts of this thesis.

The robust observation of McCloskey et al. (2007) was that Indian Ocean coasts hit hard by the December 2004 tsunami experience much smaller waves from future rupture of the Mentawai segment. To exemplify, many areas badly affected in December 2004, most notably northern Aceh Province, Thailand and eastern India experienced relatively small waves for all modeled Mentawai earthquakes.

For sites on the western coast of the Indian Ocean, this is explained by the orientation of the Mentawai segment, which results in much of the tsunami energy being directed toward the southwest, into the Southern Ocean. All simulated tsunamis propagating to the east and north are stopped by Sumatra and by its western islands. Some distant coasts, however, could expect to experience moderate wave heights. Port Headland, NWAustralia, Hambantota, Sri Lanka and the Seychelles all experience modeled waves with heights greater than 0.5 m for some of the more energetic simulations and these waves could be amplified by local bathymetric focusing to generate significant local hazards. (McCloskey et al., 2007)

Another study in which preliminary simulations were done to evaluate the transoceanic effects of a probable tsunami from West Sumatra was presented by Yalçiner et al. (2008) on COMPASS conference in Maldives. Possible rupture characteristics of an earthquake under the Mentawi Islands were defined as in 3 segments each one is 110 km length and 80 km width. Assessment analysis were done by NAMI DANCE and water level fluctuations were found around Maldivian Islands. However, in this study, since simulations were carried out at preliminary stage and according to that estimated rupture parameters were not needed to be so accurate. In the modeling studies, input parameters were estimated and the initial wave of tsunami source was computed. However, rupture

characteristic of the estimated earthquake which had been predicted and presented by McCloskey et al. (2007) and Okal and Synolakis (2007) was more devastating.

Okal and Synolakis (2007) provided the analysis of worst case scenarios of seismic rupture along the active faults based on the record of large-historical earthquakes which determine the effects of transoceanic tsunamis in Indian Ocean Basin. Ten possible case studies were defined according to the source parameters of the December 2004 Sumatra earthquake and simulations were performed by changing these parameters alternately by using the same orientation of the fault.

In this context, it is important to develop scenarios for future Indian Ocean mega-earthquakes which would generate transoceanic tsunamis capable of inflicting catastrophic levels of death and destruction in the far field. Okal and Synolakis (2007) presented hydrodynamic simulations for a number of such sources located at the subduction zones surrounding the basin and their study showed that shallow bathymetry around the epicentral area reduces the wave amplitude of tsunami in the far field.

The results of scenarios simulated by Okal and Synolakis (2007) indicated that the Maldives would be less impacted than in December 2004, due primarily to different patterns of far-field directivity in the geometries involved. The structure of the islands (steep coral atolls with relatively narrow transverse dimensions) gives the opportunity to have less tsunami runup values than on a typical shallow dipping structure. However, one should note that simulations performed by Okal and Synolakis (2007) did not include the effect of shoaling in the immediate vicinity of shorelines and of run-up on the beaches. This

problem could be solved by using site-specific high resolution models of bathymetry and topography.

As a final, it's seen from Table 1, on the 25th of October 2010, an earthquake occurred in Kepulauan – Mentawai with a magnitude of 7.80. According to International Tsunami Information Center, this earthquake caused damage and over 450 deaths in the Mentawai Islands, Indonesia. On the other hand, after this tsunamigenic earthquake, the highest measured tsunami amplitude locally was 0.35 m in Padang, Sumatra, and the highest measured amplitude overall was 0.4 m in Rodrigues Islands, Mauritius. The highest tsunami waves were reported to be 3-6 m high by eyewitnesses. (ITIC, 2010)

CHAPTER III

NUMERICAL BACKGROUND AND TSUNAMI SOURCE SELECTION

3.1. Numerical Background

This thesis focused on the numerical modeling of the worst case tsunami scenario, mentioned in Chapter 2, in Indian Ocean and the investigation of tsunami effects in Maldives. The numerical model, NAMI DANCE is used in analyses based on the necessary input data that will be described below.

NAMI DANCE is a tool, based on the solution of nonlinear form of the long wave equations with respect to related initial and boundary conditions. There were several numerical solutions of long wave equations for tsunamis; in general the explicit numerical solution of Nonlinear Shallow Water (NSW) equations is preferable for the use since it uses reasonable computer time and memory, and also provides the results in acceptable error limit.

In NAMI DANCE, for the propagation of tsunami in the shallow water, the horizontal eddy turbulence could be negligible compared to the bottom friction except for run-up on the land. The following equations which are known as Nonlinear Shallow Water (NSW) equations (3.1) are therefore given as the fundamental equations in the present model.

$$\frac{\partial \eta}{\partial t} + \frac{\partial M}{\partial x} + \frac{\partial N}{\partial y} = 0$$

$$\frac{\partial M}{\partial t} + \frac{\partial}{\partial x} \left(\frac{M^2}{D} \right) + \frac{\partial}{\partial y} \left(\frac{MN}{D} \right) + gD \frac{\partial \eta}{\partial x} + \frac{gn^2}{D^{7/3}} M \sqrt{M^2 + N^2} = 0 \quad (3.1)$$

$$\frac{\partial N}{\partial t} + \frac{\partial}{\partial x} \left(\frac{MN}{D} \right) + \frac{\partial}{\partial y} \left(\frac{N^2}{D} \right) + gD \frac{\partial \eta}{\partial y} + \frac{gn^2}{D^{7/3}} N \sqrt{M^2 + N^2} = 0$$

TUNAMI N2, developed by Profs. Shuto and Imamura and opened to the use of tsunami scientists under the umbrella of UNESCO, determines the tsunami parameters from given earthquake rupture characteristics (Imamura, 1989, Shuto, Goto, Imamura, 1990, Goto and Ogawa, 1991). It computes all necessary parameters of tsunami behavior in shallow water and in the inundation zone allowing for a better understanding of the effect of tsunamis according to bathymetric and topographical conditions. NAMI DANCE has been developed by Profs. Zaytsev, Chernov, Yalciner, Pelinovsky and Kurkin using the identical computational procedures of TUNAMI N2 (NAMI DANCE Manual v4.8, 2008). Both numerical codes are cross tested and also verified in international workshops specifically organized for testing and verifications of tsunami models (Synolakis et al., 2004, Yalciner et. al., 2007b). These models have been applied several tsunami application all over the world. As well as tsunami parameters, NAMI DANCE computes:

- tsunami source from either rupture characteristics or pre-determined wave form,
- propagation,
- arrival time,
- coastal amplification
- inundation (according to the accuracy of grid size),

- distribution of current velocities and their directions at selected time intervals,
- distribution of water surface elevations (sea state) at selected time intervals,
- relative damage levels according to drag force and impact force,
- time histories of water surface fluctuations,
- 3D plot of sea state at selected time intervals from different camera and light positions, and
- animation of tsunami propagation between source and target regions (Yalciner et. al., 2006b, 2007b).

Before making a tsunami modeling study in NAMI DANCE for a specific area, one should realize that bathymetric data is one of the most important parameter that has a direct effect on tsunami characteristics. The steps followed to produce a reliable bathymetry data were given in the next part of the report.

3.2. Bathymetry Processing

Fine gridded bathymetric data is one of the most important input parameter for numerical tsunami-modeling. This can be carried out using a dedicated research vessel with high-resolution seafloor mapping capability. GEBCO Grid Viewing and data access software is used to obtain the bathymetric data of study domain.

This thesis is mainly focused on the effects of a transoceanic or far-field tsunami triggered in Indian Ocean on Maldives by numerical modeling. For this reason the study domain was selected to cover all Indian Ocean including Maldives between the coordinates of 14° N -

7° S and 72° E - 105° E. Based on this limits, bathymetric data was accessed by using the GEBCO_08 with 30 arc-second grid.

After obtaining the bathymetric data of the study area, NAMI DANCE uses the bathymetry of the area as input data. The bathymetry of the area is usually stored as data files. This file consists of three values; x coordinate, y coordinate and the depth values. However data files are typically randomly spaced files, and this data must be converted into an evenly spaced grid before using as input file of the program. To convert into a grid file, a program called SURFER which is a contouring and 3D surface mapping program that runs under Microsoft Windows is used.

3.3. Correlation Studies

The bathymetric data obtained from GEBCO was taken in every 30 arc-second grids as the grid size is approximately 926 m. Some of the islands in Maldives, they have a width of less than 2 km. Therefore some of the islands cannot be covered in the bathymetric data since they may be located between two grid nodes. In order to solve this problem, the coordinates of the coastal borders of those islands should be determined and inserted into the present bathymetric data.

GEBCO produces planar bathymetric data which is compatible with NAMI DANCE since it covers the whole earth as if it's not spherical. However, the coordinates of islands was taken from Google Earth having spherical projection as shown in Figure 2. Thus, one should use a GIS application to convert the spherical data taken from Google Earth to the planar one to superpose bathymetric data coming from GEBCO 30 sec database.

AutoCAD Raster Design is used in this study to rubbersheet the spherical Google Earth image to the planar GEBCO data. Rubbersheeting uses a set of matched control points, consisting of source points in the image and destination points in the drawing. Specifying these points by picking them directly in the drawing, or by establishing a grid of destination points, to which source points were matched. Once these control points are established, the image is transformed so that the image file exported from Google Earth for the study area was transformed into planar projection as illustrated in Figure 3.



Figure 2. Spherical projection of the project area taken from Google Earth.

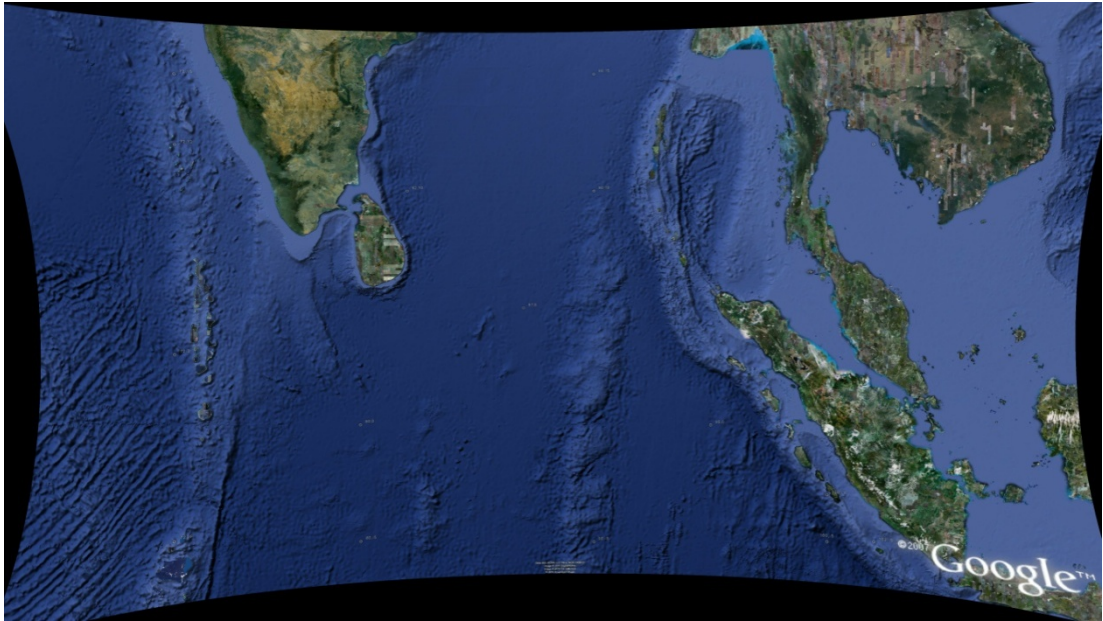


Figure 3. Planar projection of the project area transformed from spherical projection of Google Earth by AutoCAD Raster Design.

After obtaining planar projection map, the small islands that cannot be covered by GEBCO are manually digitized by using SURFER. In order to do digitization in more accurate way, the study area is divided into four regions as B, C, D and E in a nested manner to have a much better focus on the Maldives Islands. The coverage area by each domain will be explained and demonstrated in the following chapter of this report. Having defined the regions, starting from the E, the smallest region, the bathymetric data taken from GEBCO and the planar projection map obtained from Google Earth were superimposed and then manually digitized data was completed by defining elevations of coastal border and land areas. The coordinates of selected points on coastal border and land areas, together with the corresponding elevations, were inserted into the bathymetry file.

3.4. Tsunami Source Selection

Since the earthquake triggered tsunamis were mainly investigated, tsunami source selection studies had become crucially significant for making a reliable model in this thesis. A certain number of studies had been carried out to find a probable failure model for the stress field in the Sumatra zone of Sunda arc. Methodically, throughout many studies to examine the robustness of the computational algorithms, before modeling possible future tsunami scenarios, the simplified models of previous events were examined. In this thesis the 2004 Sumatra – Andaman earthquake is studied as the first case. Sumatra - Andaman earthquake source parameters, defined by Earth Sciences Department and Institute of Geophysics and Planetary Physics of University of California were used and it's given in Table 2. The generation of the first wave and corresponding water surface elevation are demonstrated in Figure 4. In tsunami simulations performed by Lay et al. (2005), these parameters were already used and provided a satisfactory fit to the satellite observations.

Table 2. Rupture characteristics of the Sumatra-Andaman earthquake, 2004, (Lay et al., 2005)

	Segment I	Segment II	Segment III
Epicenter	94E-2.5N	91E-5.5N	89.9E-8.6N
Length of fault (km)	420	325	570
Strike angle (deg. CW)	315	345	10
Width of fault (km)	240	170	160
Focal depth (km)	10	10	10
Dip angle (deg.)	10	15	18
Rake angle (deg.)	110	120	140
Slip displacement (m.)	20	5	2
Height of maximum positive amplitude(m.)	7.82		

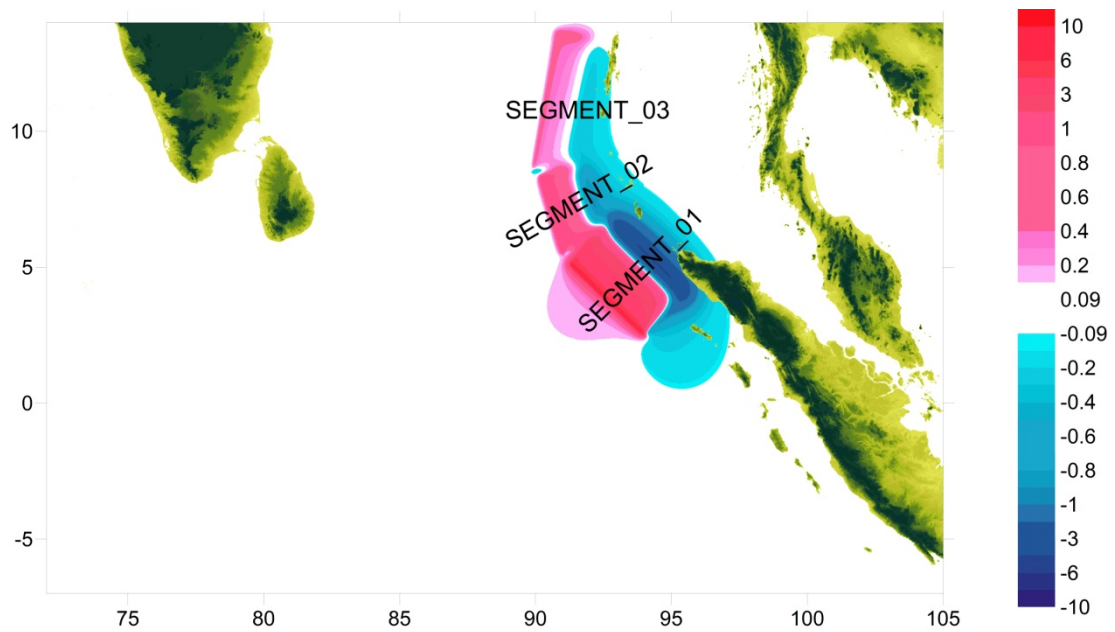


Figure 4. Initial water surface elevation for the Sumatra-Andaman earthquake, 2004

According to the Nalbant and Pollitz in McCloskey et al. (2005), megathrust under the Batu and Mentawai Islands could be expected to fail due to the increased stress field by the Sumatra-Andaman earthquake. Furthermore, in the frame of paleogeodetic studies, it had been shown that the megathrust under the Batu Islands was slipping at about the rate of plate convergence (Natawidjaja et al., 2004) while under Siberut Island it had been locked since the great 1797 earthquake and had recovered nearly all the strain released then (Natawidjaja et al., 2006). This situation makes it clear that, the megathrust under the Batu and Mentawai Islands is in its seismic cycle and may initiate the interaction stress triggering (McCloskey et al., 2007). In the light of this information, although it seemed to be unexpected, 800-km long rupture scenario extending from beneath Siberut Island through the Enganno region to the Sunda Strait had been selected as a worst case by McCloskey et al. (2007) as, full range of possible tsunami threats to the Sumatran coast was investigated in their study. The mentioned worst case scenario by McCloskey et al.

(2007) here is to be studied as the second case and generation of the first wave is illustrated at Figure 5. The source parameter of the earthquake is given in Table 3.

Table 3. Rupture characteristics of the earthquake selected as the second case.
(McCloskey et al., 2007)

Epicenter	102.1 E – 6 S
Length of fault (km)	800
Strike angle (deg. CW)	320
Width of fault (km)	180
Focal depth (km)	10
Dip angle (deg.)	15
Rake angle (deg.)	110
Slip displacement (m.)	10
Height of maximum positive amplitude (m.)	4.27

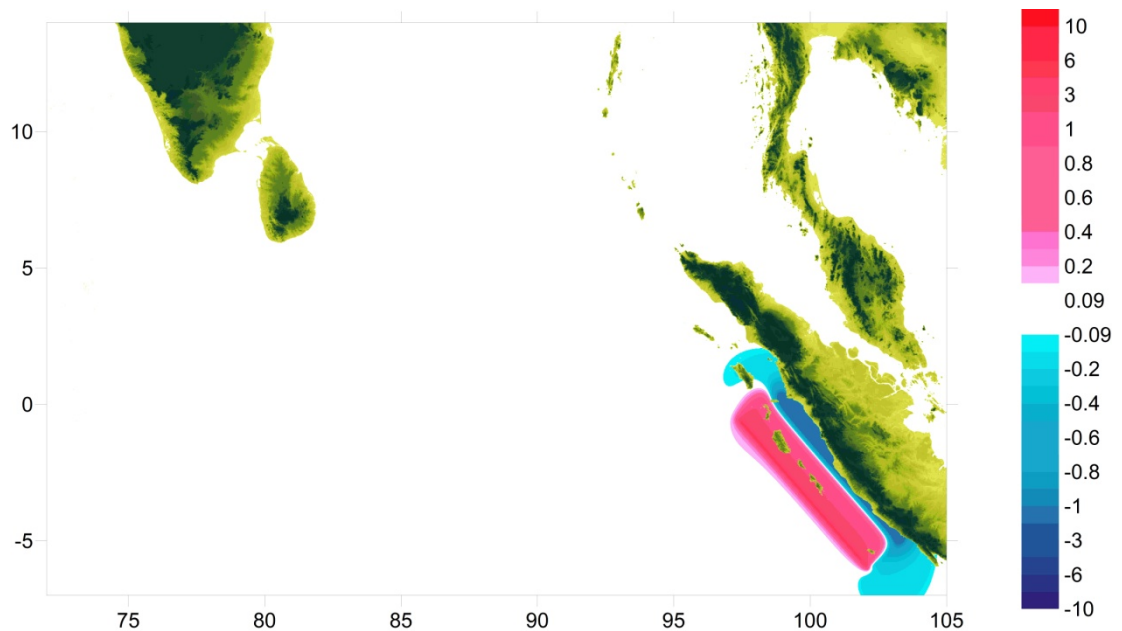


Figure 5. Initial water surface elevation for the second case. (McCloskey et al., 2007)

Another simulation study in the literature was offered by Okal and Synolakis (2007) to assess the far-field tsunami hazard in the Indian Ocean basin. In their study, active seismic zones around the Indian Ocean were emphasized and according to these zones ten case studies of possible earthquakes were modeled and their scenarios were shown in Figure 6. In their simulations, the worst-case scenarios which had been triggered by the seismic rupture along the faults having supported large earthquakes in the historical record were defined. Among other scenarios, Scenario 2 was considered as simply the repeat of the great earthquake of 1833 with one difference. The length of fault were extended to 900km along the southeast direction in their model and that makes that scenario as the most hazardous one in terms of Maldives and Madagascar since it caused the wave amplitudes to increase as high as seven times those of observed in December 2004 along the east coast of Madagascar.

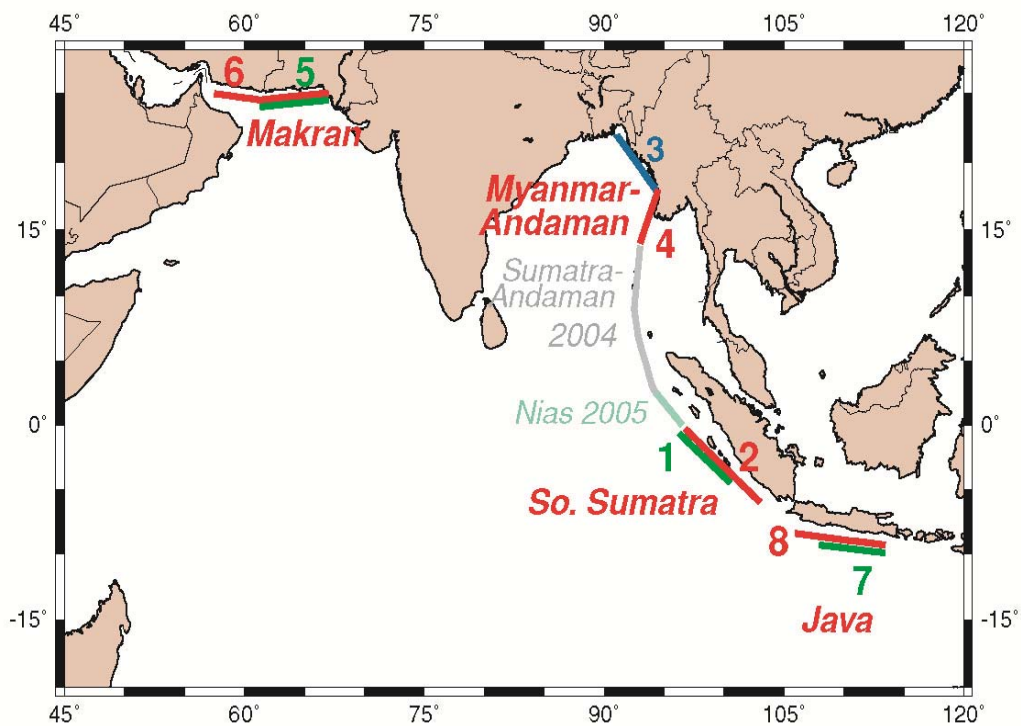


Figure 6. Map of tsunamigenic earthquake scenarios. (Okal and Synolakis, 2007)

Being considered as the worst scenario, in Okal and Synolakis (2007)'s also claims Scenario 2 to be low in likelihood due to the occurrence of the Bengkulu earthquake in 2007. In order to strengthen their argument, Okal and Synolakis (2007) carefully investigated 2004 Sumatra–Andaman earthquake and 1881 Car-Nicobar earthquake. Their studies show that, 1881 earthquake was not an effective barrier since the 2004 earthquake was initiated and extended over it with a lesser convergence rate. In that manner, in same study, Scenario 2a was more realistically defined to be a long fault inspired from Scenario 2, but with an average slip reduced to 8 m. to take into account the partial strain release in its northern segment during the 2007 Bengkulu event. Being significantly probable, in this thesis, the Scenario 2a of Okal and Synolakis (2007) was to be studied as the third case. The related source parameter of Scenario 2a and generation of the first wave are given in Table 4 and Figure 7.

Table 4. Rupture characteristics of the earthquake selected as the third case. (Okal and Synolakis, 2007)

Epicenter	102.46 E – 6.9 S
Length of fault (km)	900
Strike angle (deg. CW)	322
Width of fault (km)	175
Focal depth (km)	10
Dip angle (deg.)	12
Rake angle (deg.)	90
Slip displacement (m.)	8
Height of maximum positive amplitude (m.)	3.38

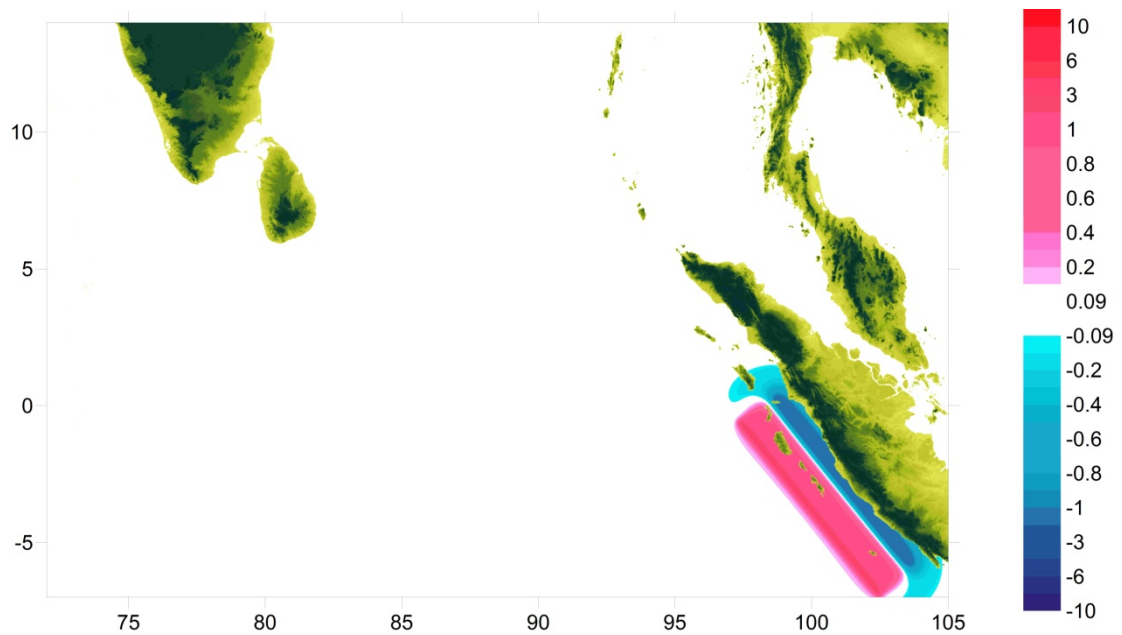


Figure 7. Initial water surface elevation for the third case. (Okal and Synolakis, 2007)

3.5. Selection of Gauges

Gauges are certain locations in a study domain, especially selected near the coast line in order to analyze the time histories of water surface fluctuations. In this thesis, gauge points were selected according to the populated areas in Maldives, since the effects of far-field tsunamis on Maldives were one of the main focuses of studies. The coordinates of gauge locations which were primarily used in the analysis are given in Table 5. Apart from these gauges, some other gauges points were randomly placed to analyze the wave propagation in deep ocean. The location of all gauge points and their distributions in the study area are marked in Figure 8.

Table 5. Coordinates of selected gauge points.

Gauge #	Longt.	Lat.	Gauge #	Longt.	Lat.
A1	73.53667	4.252133	PADANG	100.0833	-0.6
A2	73.53913	4.252133	SIBOLGA	98.71667	1.733333
B1	73.52866	4.211469	SHAVIYANI	73.15	6.316667
B2	73.53236	4.211469	OLIVEFUSHI	73.60559	5.294471
C1	73.52496	4.180664	DONVELI	73.55	4.25
C2	73.52743	4.180664	KANDOOMA	73.45	3.883333
D1	73.5342	4.18	VEVARU	73.60559	2.96875
D2	73.53297	4.180047	THAA	73.35	2.383333
E1	73.54159	4.19545	LAAMU	73.54115	1.9119
E2	73.54036	4.19545	FUVAMMULAH	73.251	0.216667
F1	73.54406	4.2053	HULHUDU	73.21667	-0.58333
F2	73.54344	4.205308	GAN	73.45	-0.31667
G1	73.54899	4.215782	HULHUMEEDHO	73.21667	-0.63333
G2	73.54714	4.215782	GURADU	73.58533	5.433333
H1	73.55083	4.228104	DIFURI	73.352	5.433333
H2	73.55022	4.227488	DHIFUSHI	73.652	4.516667
I1	73.55391	4.239194	MULI	73.58957	2.932692
I2	73.5533	4.239194	MAVARU	73.552	0.4
J1	73.52188	4.173886	TIDE HANIMAADOO	73.17	6.74
J2	73.51942	4.1745	TIDE GAN	73.16	-0.68
K1	73.52188	4.183128	TIDE MALE	73.54	4.18
K2	73.5194	4.183128	FUJIMA01	73.5319	4.19056
L1	73.50525	4.181896	FUJIMA02	73.5328	4.18917
L2	73.50587	4.18066	FUJIMA03	73.535	4.18917
M1	73.50156	4.17512	FUJIMA04	73.5375	4.19028
M2	73.5022	4.17512	FUJIMA05	73.5408	4.20111
N1	73.51326	4.16896	FUJIMA06	73.5446	4.21661
N2	73.51326	4.169574	FUJIMA07	73.5453	4.21617

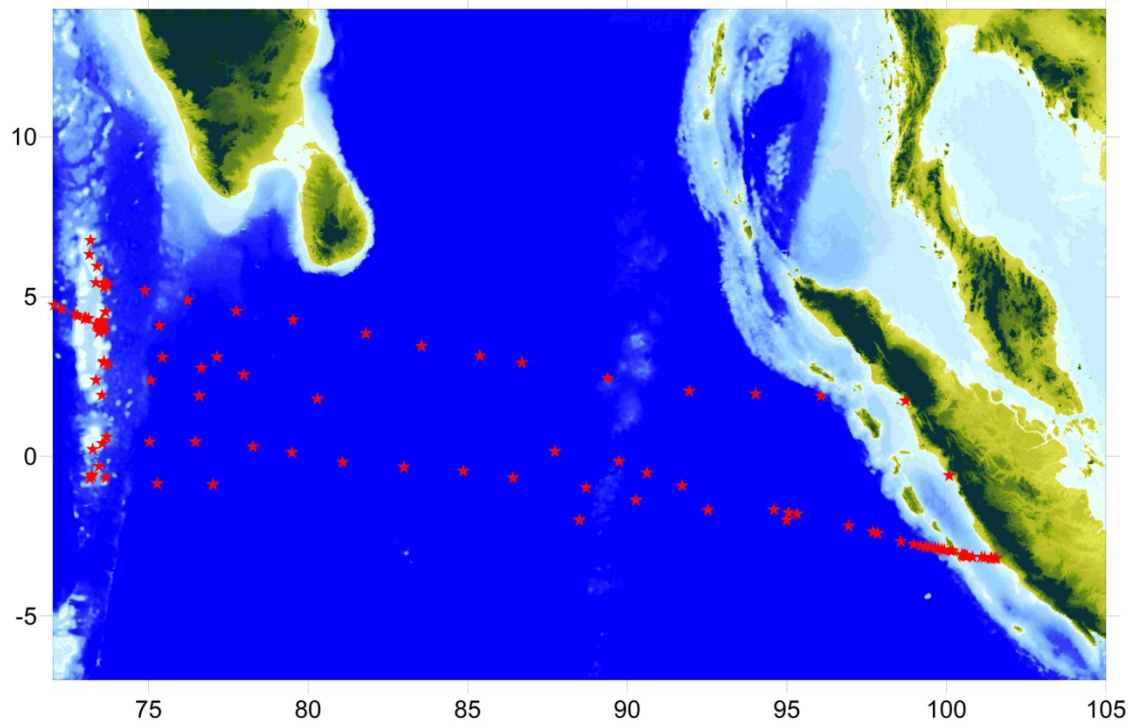


Figure 8. Location and distribution of selected gauge points.

CHAPTER IV

MODELLING STUDIES

The rupture parameters given in Table 2, 3 and 4 were used to determine the tsunami source in simulations. Duration of the simulations was taken as 600 minutes. The results of the simulations are given in the following part of this chapter. The software called as SURFER was used in order to plot the maximum and minimum values for each grid. Furthermore, GRAPHER was also used in the drawings of the time histories of water surface fluctuations.

4.1. Domain Selection

In modeling study, since, the main purpose of this thesis is the effect of far-field tsunamis on Maldives Islands, lies on the small portion of the study area, the simulations of the all scenarios were done in a nested manner in order to come up with more accurate results. For this reason, the largest domain was defined as “Domain B” and in that domain three different sub-domains were defined as “Domain C, D and E”. Selected domains are shown on Figure 9 and the coordinates of the corresponding bounding area for all domains are given in Table 6. The grid size, which is the distance between two grids of the bathymetry file, were determined as 1850 m., 616.7 m., 205.6 m. and 68.5 m. for Domain B, C, D and E respectively.

Table 6. Boundary coordinates of domains.

Domain #	Longt.	Lat.
Domain B	72.000 E – 105.000 E	7.000 S – 14.000 N
Domain C	72.430 E – 74.100 E	1.000 S – 7.280 N
Domain D	73.300 E – 73.750 E	4.120 N – 4.500 N
Domain E	73.480 E – 73.565 E	4.140 N – 4.270 N

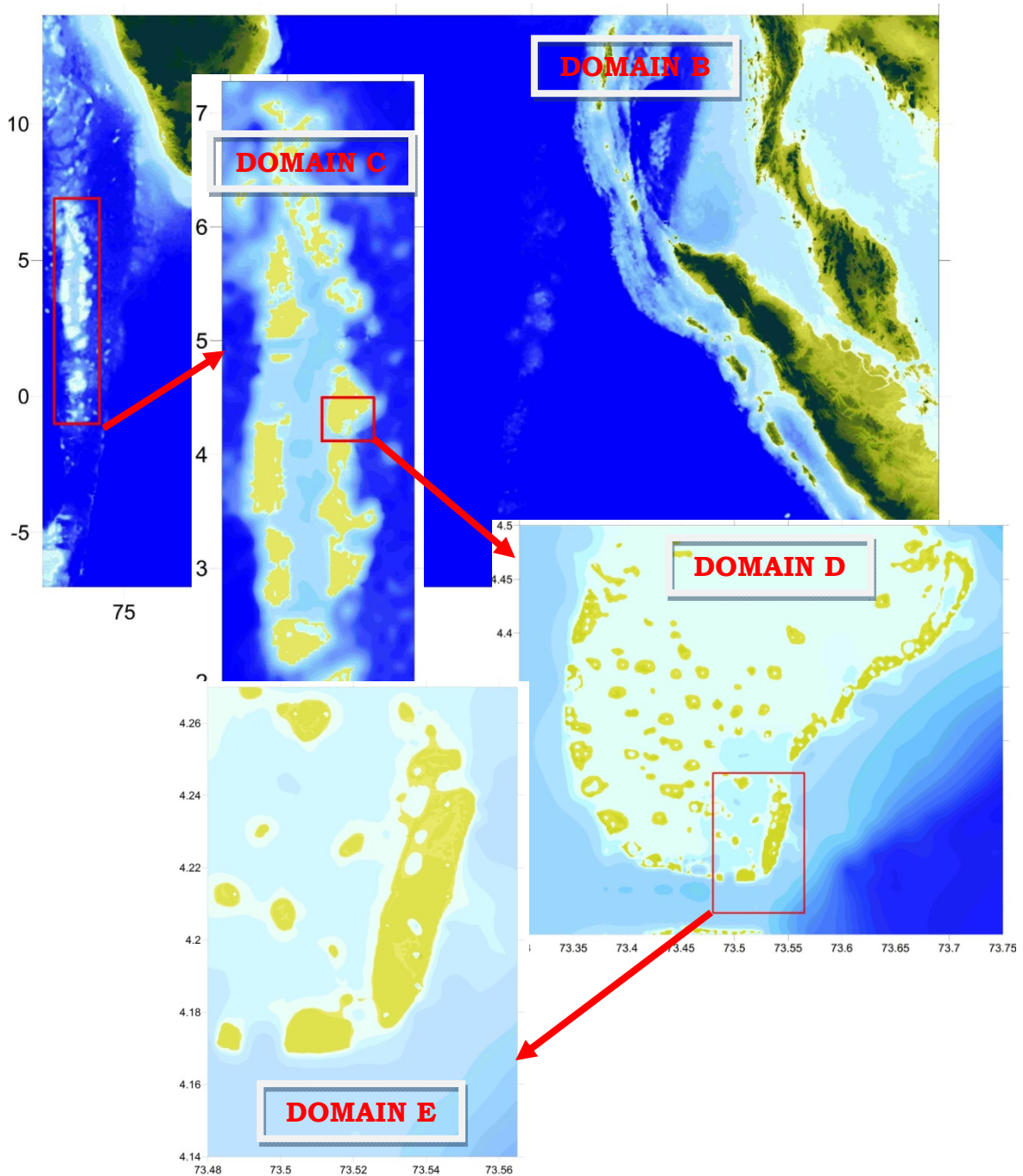


Figure 9. Demonstration of selected domains for nested analysis.

4.2. Propagation of Tsunamis

The modeling studies for the propagation of tsunamis were performed based on the rupture parameters of three different scenarios which are given in Table 2, 3 and 4. The simulation results for each case are given in the following in respective sections for selected gauges in Figure 10.

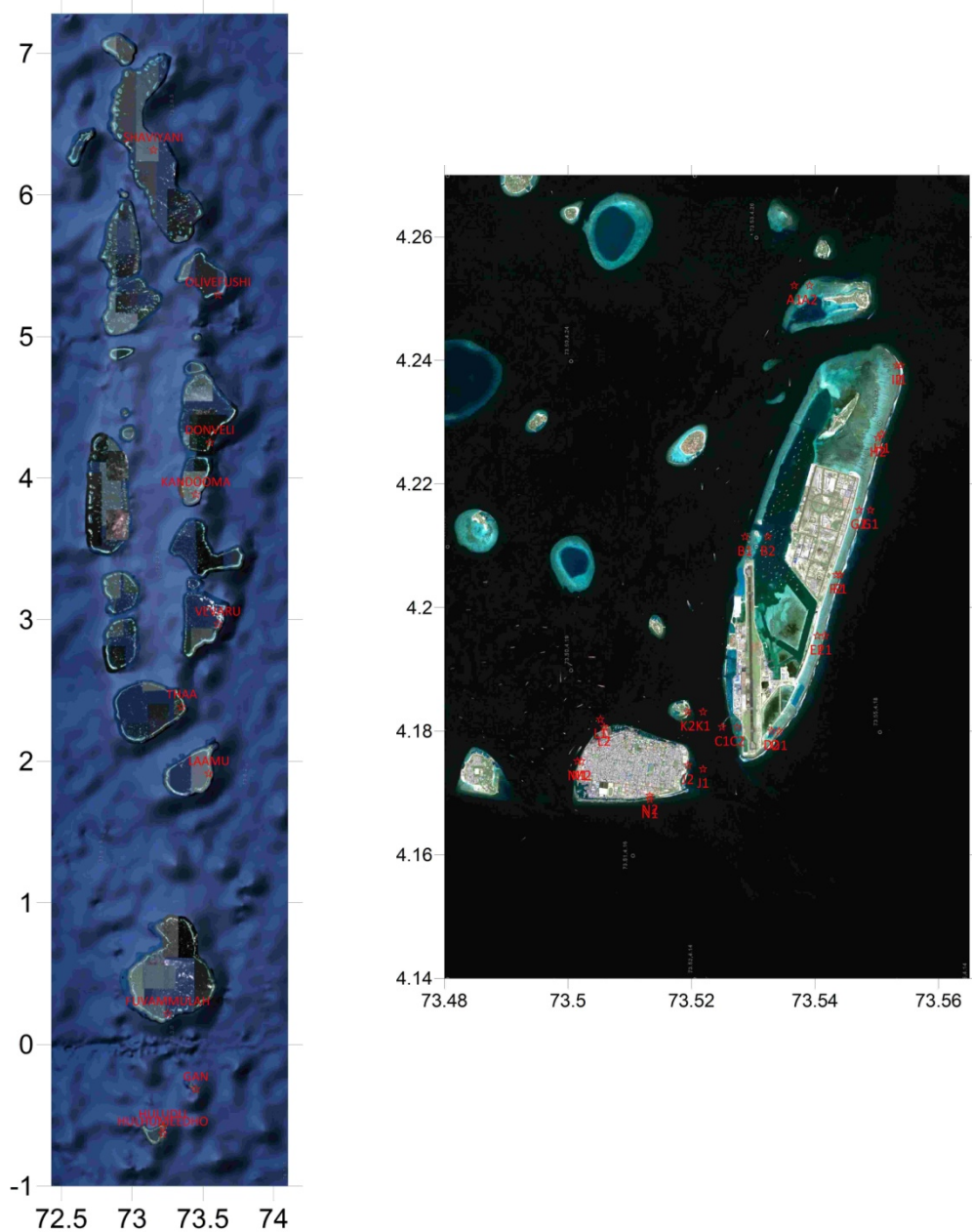


Figure 10. Gauges located at Maldives Islands in Domain C and E.

4.2.1. Sumatra-Andaman Earthquake, 2004

At first, to verify the stability and validity of modeling studies, a simplified model of a well-known past event was considered. In that manner 2004 Sumatra-Andaman earthquake was modeled and the arrival time of first wave is demonstrated in Figure 11. The tsunami source defined by Earth Sciences Department and Institute of Geophysics and Planetary Physics of University of California was used (Lay et al., 2005). In Figure 12, the propagation and arrival time of maximum wave are presented.

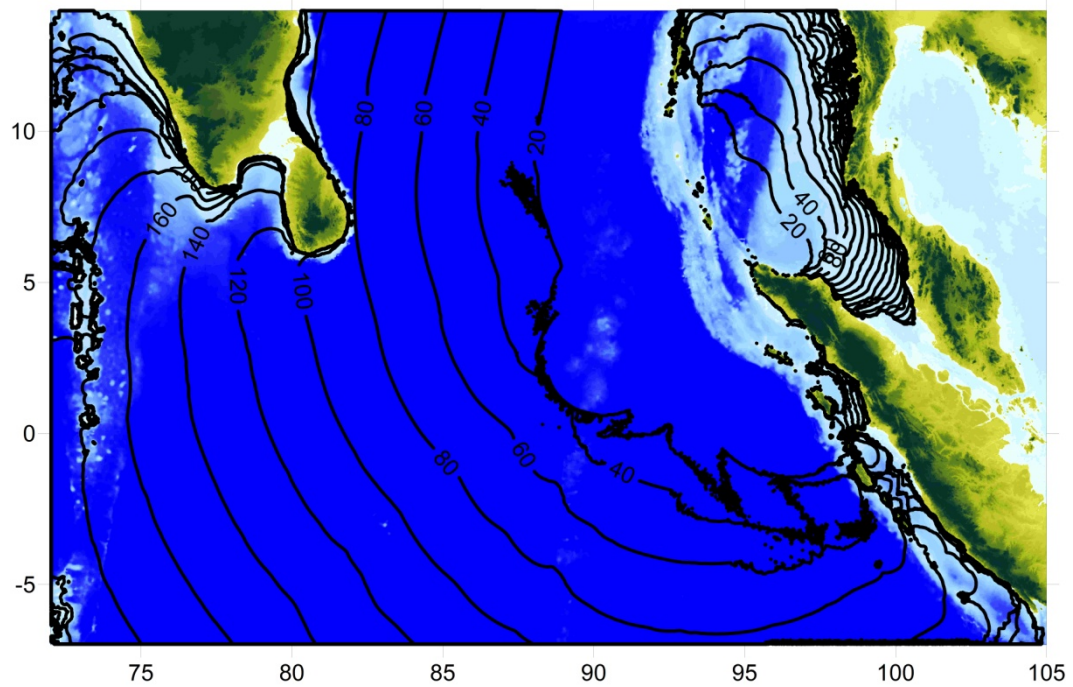


Figure 11. Arrival time of first wave for Sumatra-Andaman earthquake, 2004.

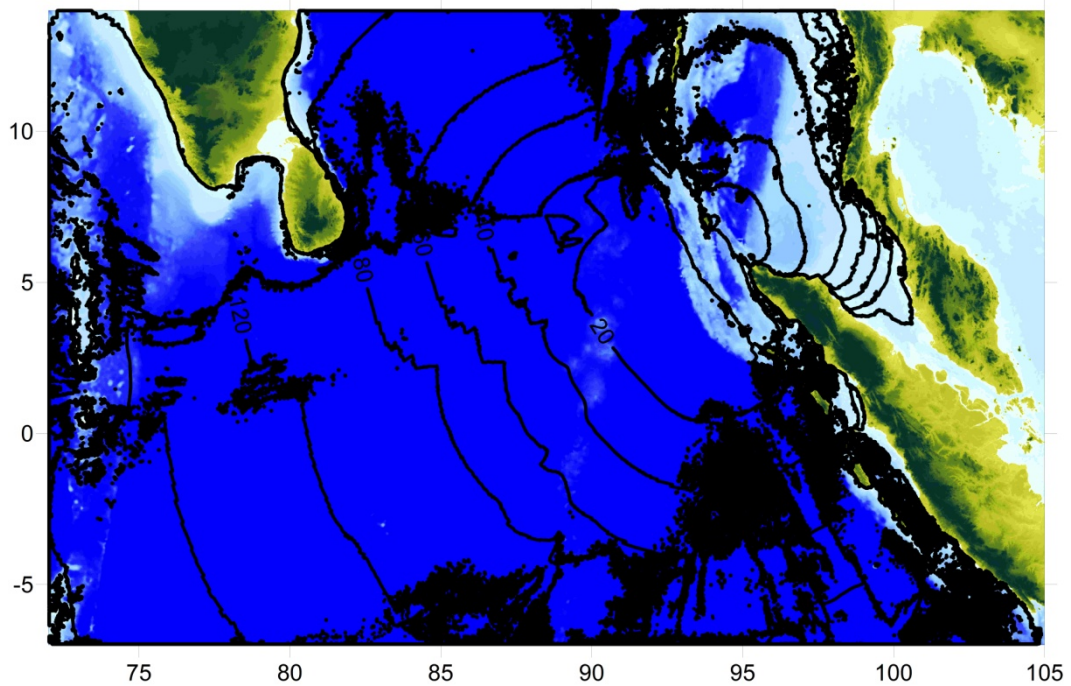


Figure 12. Arrival time of the maximum wave for Sumatra-Andaman earthquake, 2004.

As it's seen from Figure 11, the arrival time of the first wave to Maldives was about 170 minutes. On the other hand (Figure 12), the maximum wave is arrived between 170 and 270 minutes.

Sea state at 0, 60, 120, 180, 240, 300, 360, 420, 480 and 540 minutes are presented in Figures 13 and Figure 14. In all the figures, positive and negative wave amplitudes are shown by tones of red and blue colors respectively.

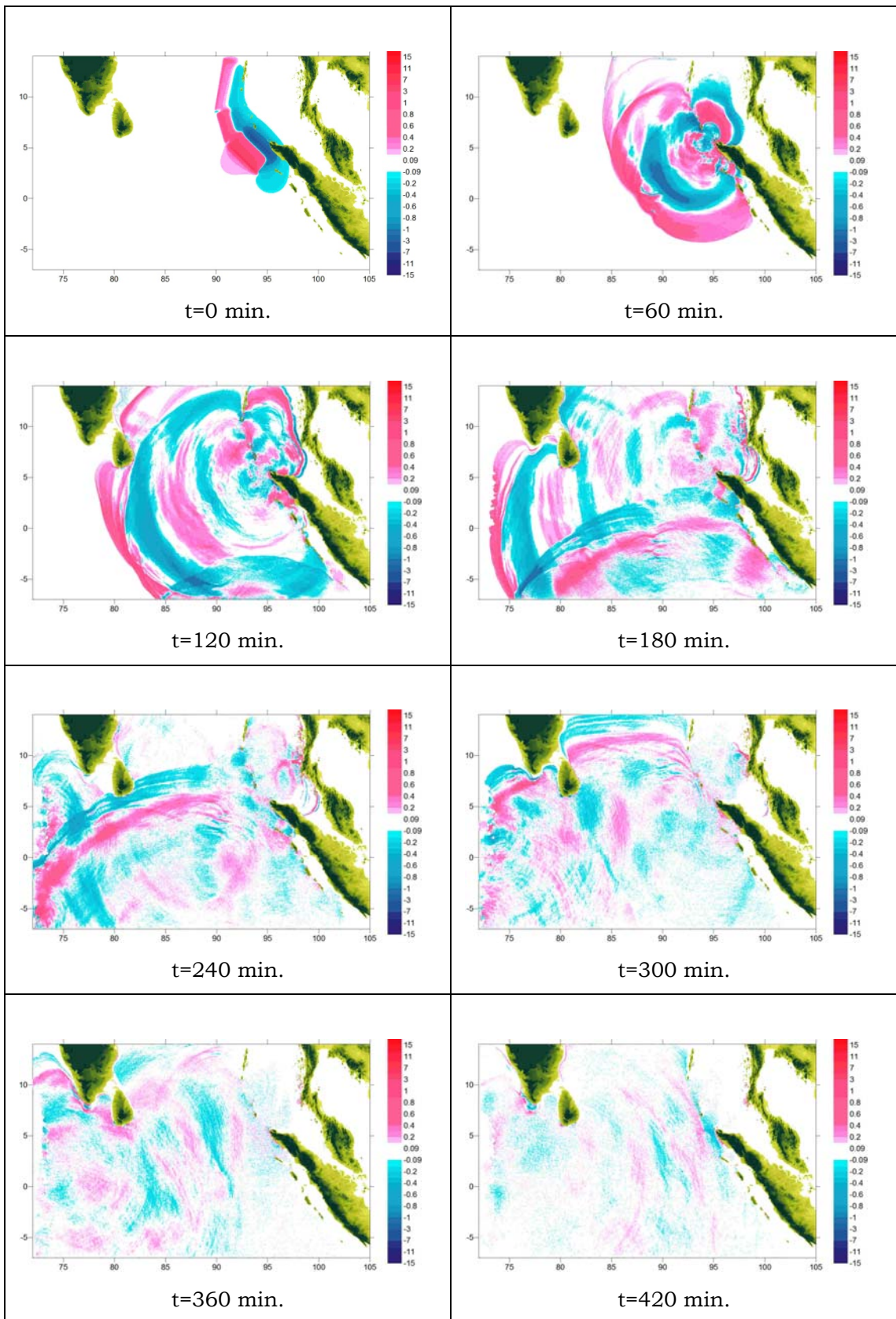


Figure 13. Sea states between $t=0$ and $t=420$ min. for Sumatra-Andaman earthquake, 2004.

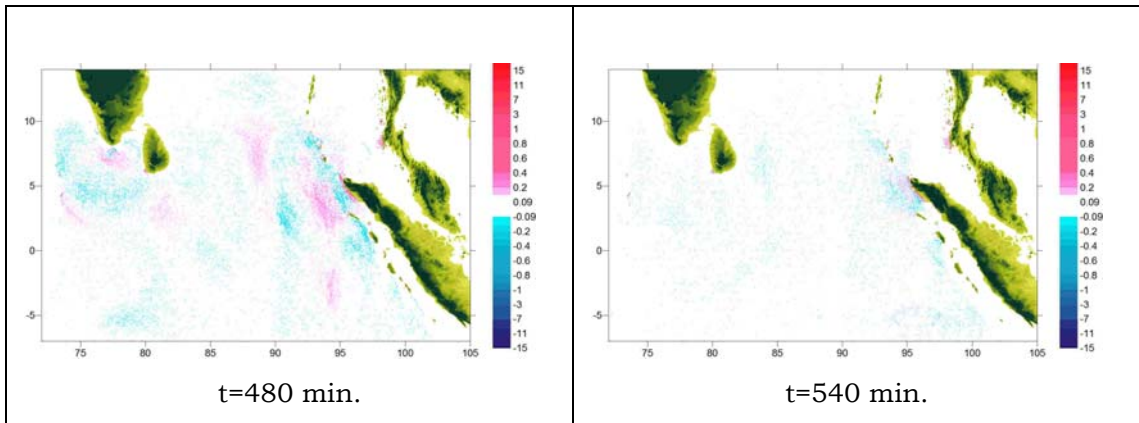


Figure 14. Sea states between $t=480$ and $t=540$ min. for Sumatra-Andaman earthquake, 2004.

The maximum positive and negative wave amplitudes in Domain C and E are computed and plotted in Figure 15 and 16.

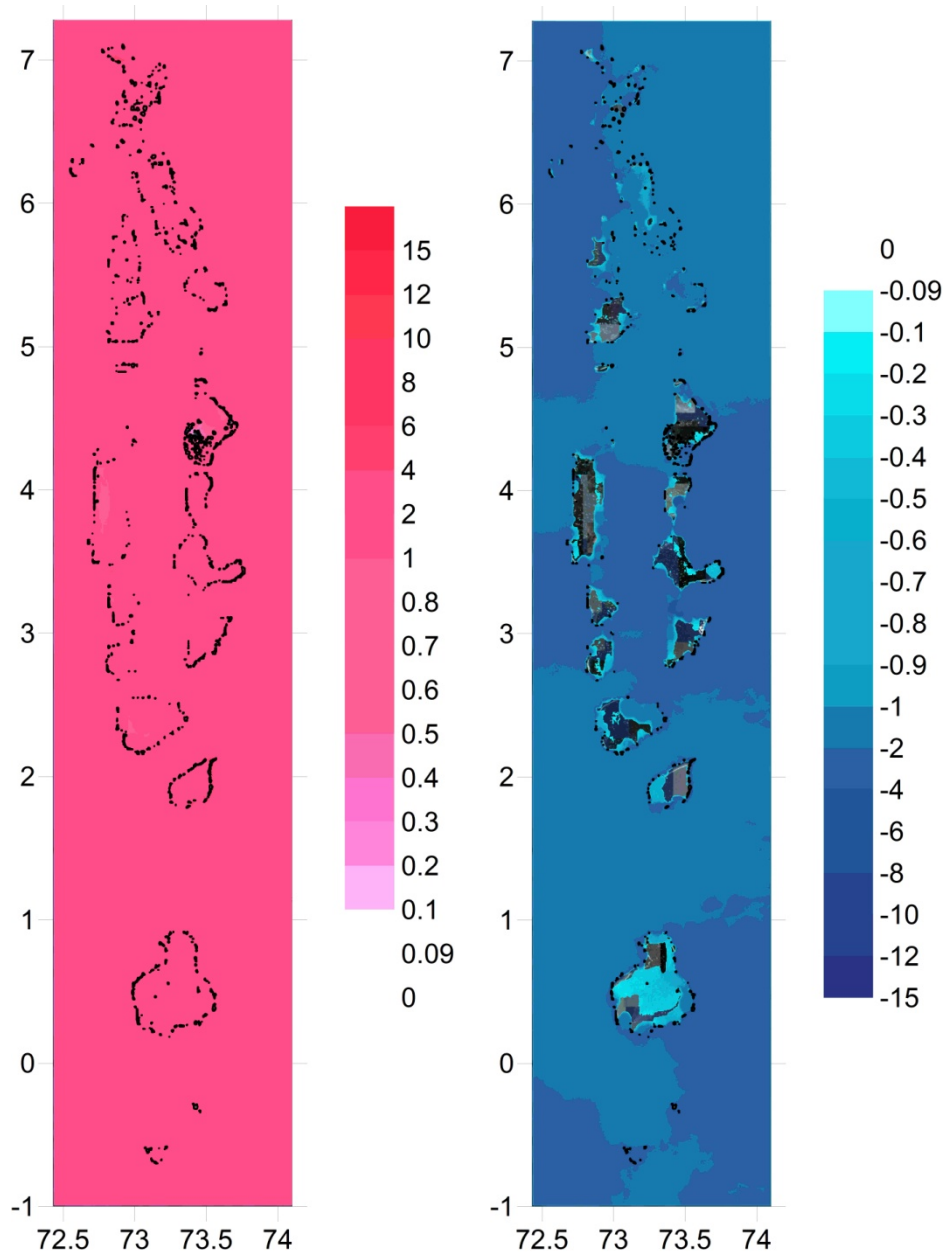


Figure 15. Maximum positive and negative wave amplitudes in Domain C for Sumatra-Andaman Earthquake, 2004.

Table 7. Results of simulation study in Domain C for Sumatra-Andaman earthquake, 2004.

Name Of Gauge	Depth Of Gauge (m)	X Coord	Y Coord	Arrival Time Of First Wave (min)	Arrival Time Of Max. Wave (min)	Maximum (+) Wave Amp.(m)	Maximum (-) Wave Amp.(m)
Shaviyani	8.9	73.15	6.31667	176	291	2.0	-0.4
Olivefushi	15.6	73.6056	5.29447	170	278	2.2	-1.4
Donveli	2.3	73.55	4.25	169	171	3.3	-2.3
Kandooma	4.1	73.45	3.88333	170	275	2.5	-1.6
Vevaru	5.6	73.6056	2.96875	168	169	2.1	-1.3
Thaa	9.0	73.35	2.38333	170	189	2.5	-1.5
Laamu	14.6	73.5412	1.9119	169	173	6.0	-3.4
Fuvammulah	5.6	73.251	0.216667	170	185	2.5	-1.8
Hulhudu	8.3	73.2167	-0.583333	171	181	2.9	-1.5
Gan	8.9	73.45	-0.316667	169	231	2.8	-2.6
Hulhumeedho	18.3	73.2167	-0.633333	171	337	3.1	-2.3
Guradu	1.5	73.5853	5.43333	174	277	1.8	0.0
Difuri	1.1	73.352	5.43333	175	313	2.0	0.0
Muli	2.3	73.5896	2.93269	169	270	1.9	-0.3
Mavaru	1.1	73.552	0.4	169	236	1.9	0.0

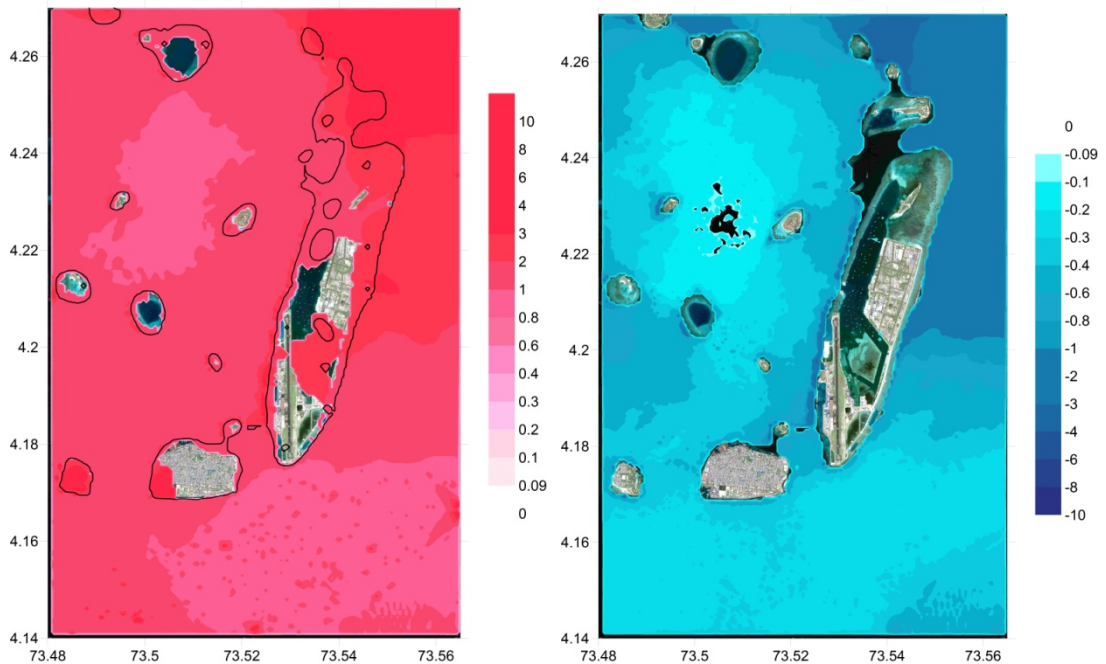


Figure 16. Maximum positive and negative wave amplitudes in Domain E for Sumatra-Andaman Earthquake, 2004.

Table 8. Results of simulation study in Domain E for Sumatra-Andaman earthquake, 2004.

Name Of Gauge	Depth Of Gauge (m)	X Coord	Y Coord	Arrival Time of First Wave (min)	Arrival Time of Max. Wave (min)	Maximum (+)Wave Amp.(m)	Maximum (-)Wave Amp.(m)
A1	6.2	73.5367	4.25213	168	170	1.9	-0.6
B1	5.8	73.5287	4.21147	168	178	2.4	-0.7
C1	7.5	73.525	4.18066	168	171	1.3	-0.6
D1	4.9	73.5342	4.18	168	267	1.3	-0.5
E1	8.1	73.5416	4.19545	168	267	1.8	-1.1
F1	8.3	73.5441	4.2053	168	267	2.2	-1.4
G1	9.3	73.549	4.21578	168	216	2.9	-2.1
H1	4.6	73.5508	4.2281	168	170	2.8	-1.6
I1	7.7	73.5539	4.23919	168	170	2.9	-1.5
J1	8.1	73.5219	4.17389	168	273	1.1	-0.4
K1	7.1	73.5219	4.18313	168	274	1.3	-0.6
L1	5.3	73.5053	4.1819	168	173	1.5	-0.4
M1	7.9	73.5016	4.17512	168	171	1.2	-0.4
N1	8.3	73.5133	4.16896	168	171	1.3	-0.5
A2(at land)	-1.0	73.5391	4.25213	169	170	2.4	0.0
B2(at land)	-1.0	73.5274	4.18066	171	171	1.0	0.0
C2(at land)	-1.0	73.5404	4.19545	168	268	1.7	0.0
D2(at land)	-1.1	73.5434	4.20531	168	267	2.4	0.0
E2(at land)	-1.0	73.5194	4.1745	171	274	1.4	0.0
F2(at land)	-1.0	73.5194	4.18313	171	171	1.3	0.0
G2(at land)	-1.1	73.5059	4.18066	171	173	1.6	0.0
H2(at land)	-1.2	73.5022	4.17512	171	429	2.0	0.0

The maximum positive and negative wave amplitudes at selected gauge points in Domain E are found to be 2.9 m. and -2.1 m. respectively.

Keating and Helsley (2005) states that, according to the reported tsunamis, triggered wave height changes between 61 cm. and 249 cm on Maldives Islands. To be consistent with Keating and Helsley, some

gauges were placed on the land side to make an evaluation of the modeling study. The gauges located on the island are shown in Table 8 with minus depth values. In modeling study, tsunami heights at these gauges are measured to be between 100 cm. and 240 cm. Here, it can be clearly seen that the maximum water elevations computed in this study for 2004 event is in similar order with the site observation given in Keating and Helsey (2005). Although depending on the observational data which is arguably acceptable in scientific terms, the results seem valid and consistent with the effects of Sumatra-Andaman earthquake, 2004.

Apart from the site investigation handled by Keating and Helsey (2005), the recorded data of tide gauges in Indian Ocean is also available. These recorded observations of tide gauges are very useful measurements to make a comparison with the simulation results. Merrifield et al. (2005) studied on the tide gauge measurements of Indian Ocean tsunami which was triggered by the Sumatra-Andaman earthquake on 26th December 2004 and according to him, tide gauge recordings, during this earthquake, in Hanimaadoo, Male, and Gan islands are given in Table 9. In this table, in order to make a comparison with the recorded measurements, our simulation study results for the gauge stations around Hanimaadoo, Male and Gan islands are also given. Furthermore, time history graphs of these gauges were taken from National Oceanic and Atmospheric Administration and it's illustrated in Figure 17.

Table 9. Tide gauge observations (Merrifield et al., 2005) and computed maximum positive wave amplitudes.

Tide Gauge	Tide Gauge Recordings, Merrifield et al. (2005)	Modelled as the 1 st Case, Sumatra-Andaman Earthquake, 2004
	Maximum (+) Wave Amp.(m)	Maximum (+) Wave Amp.(m)
Hanimaadoo	1.71	2.00
Male	1.46	1.85
Gan	0.88	1.46

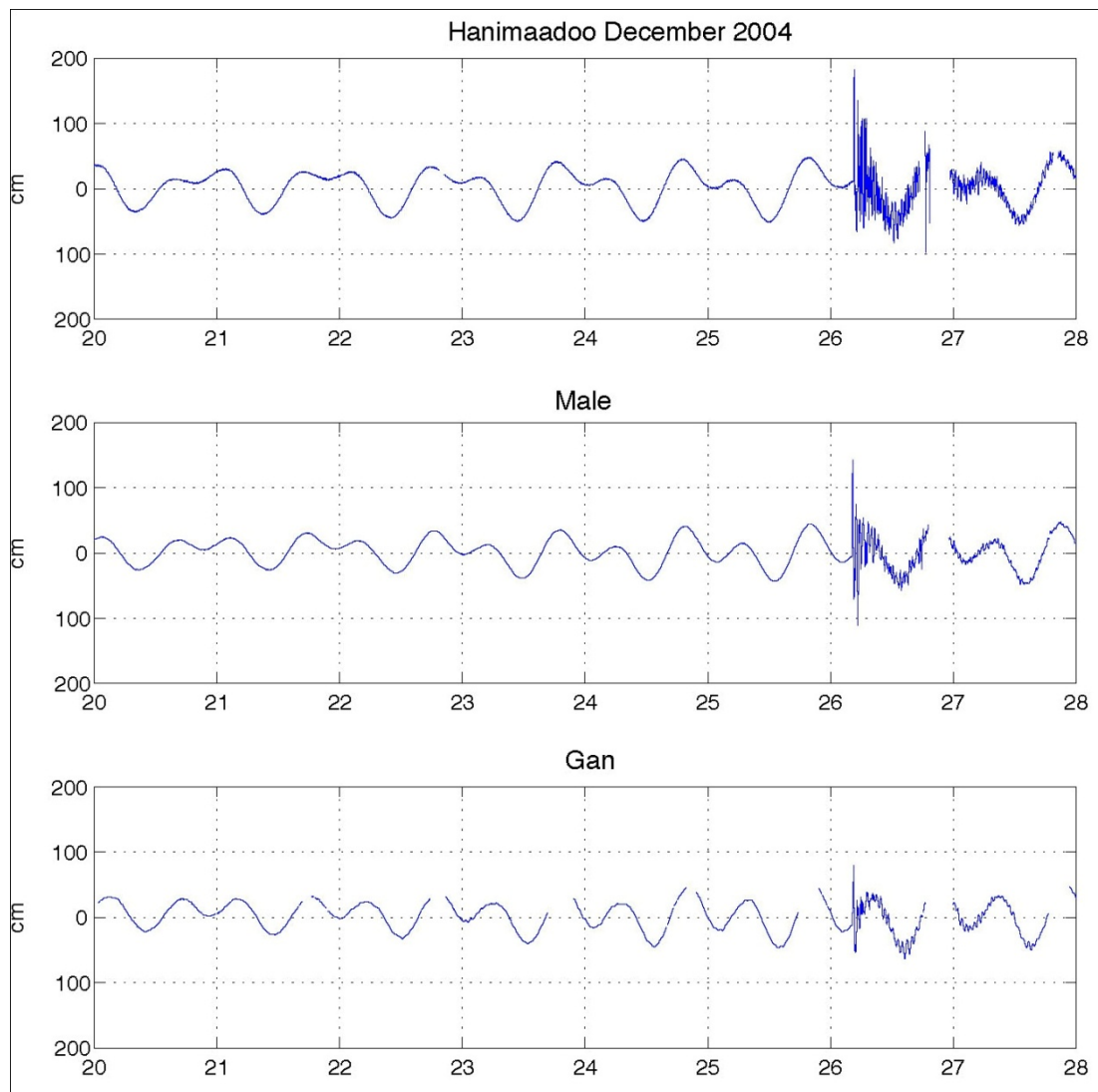


Figure 17. Tide gauges record in Hanimaadoo, Male and Gan islands during 26th December 2004 Sumatra-Andaman earthquake. (Based on NOAA, USA)

Based on the given simulation results in Table 9, although, the computed values are a little bit higher than the measured one, in general perspective, computed and recorded values are compatible with each other and simulations could be performed to estimate the risk of potential future tsunamis. The difference between the computed and recorded values is actually caused by the uncertainty in the exact location and wide sampling interval of tide gauges.

4.2.2. Megathrust under the Batu and Mentawai Islands (McCloskey et al., 2007)

According to the second case which was already defined in the tsunami source selection part of this thesis, arrival time of initial wave and the wave which had the maximum amplitude are illustrated in Figure 18 and Figure 19.

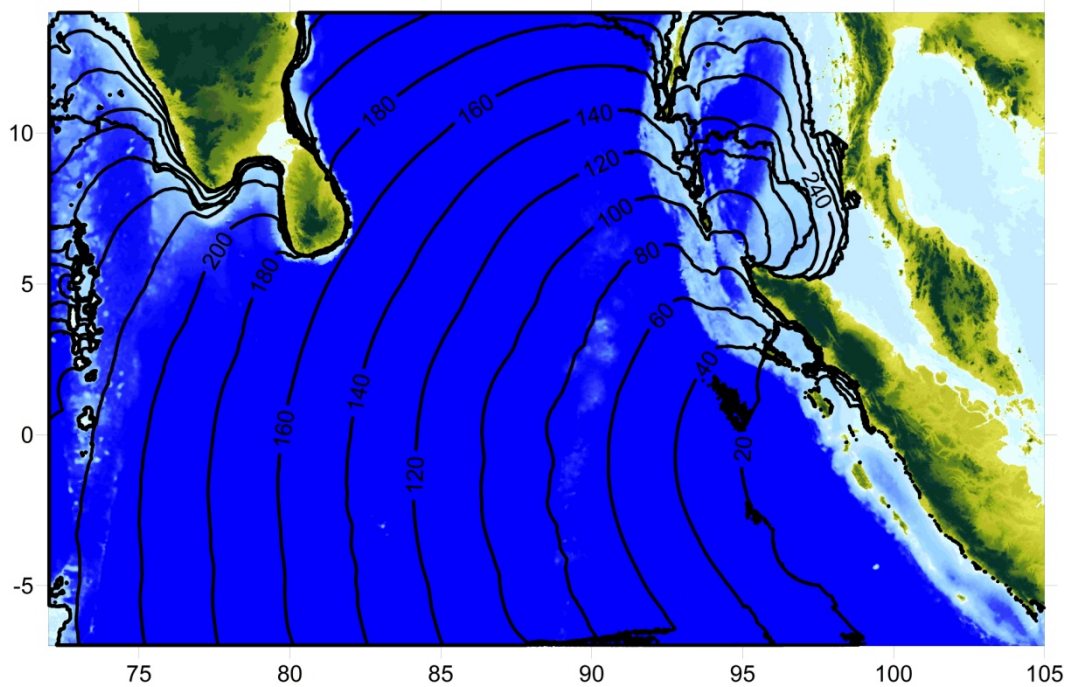


Figure 18. Arrival time of first wave for the 2nd case. (McCloskey et al., 2007)

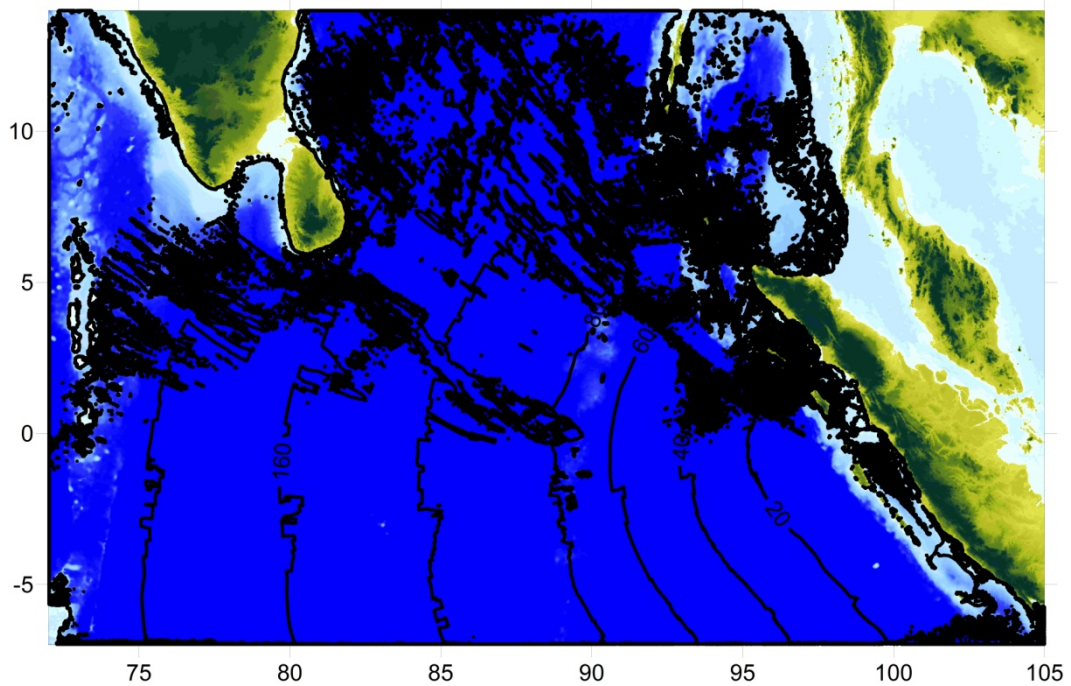


Figure 19. Arrival time of the maximum wave for the 2nd case. (McCloskey et al., 2007)

The arrival time of the first wave, based on the second case, as shown on Figure 18 to Maldives is about 230 minutes. On the other hand, the maximum wave is arrived about 40 minutes later after the arrival of the first wave (Figure 19). Sea state for 0, 60, 120, 180, 240, 300, 360, 420, 480 and 540 minutes are illustrated in Figures 20 and Figure 21.

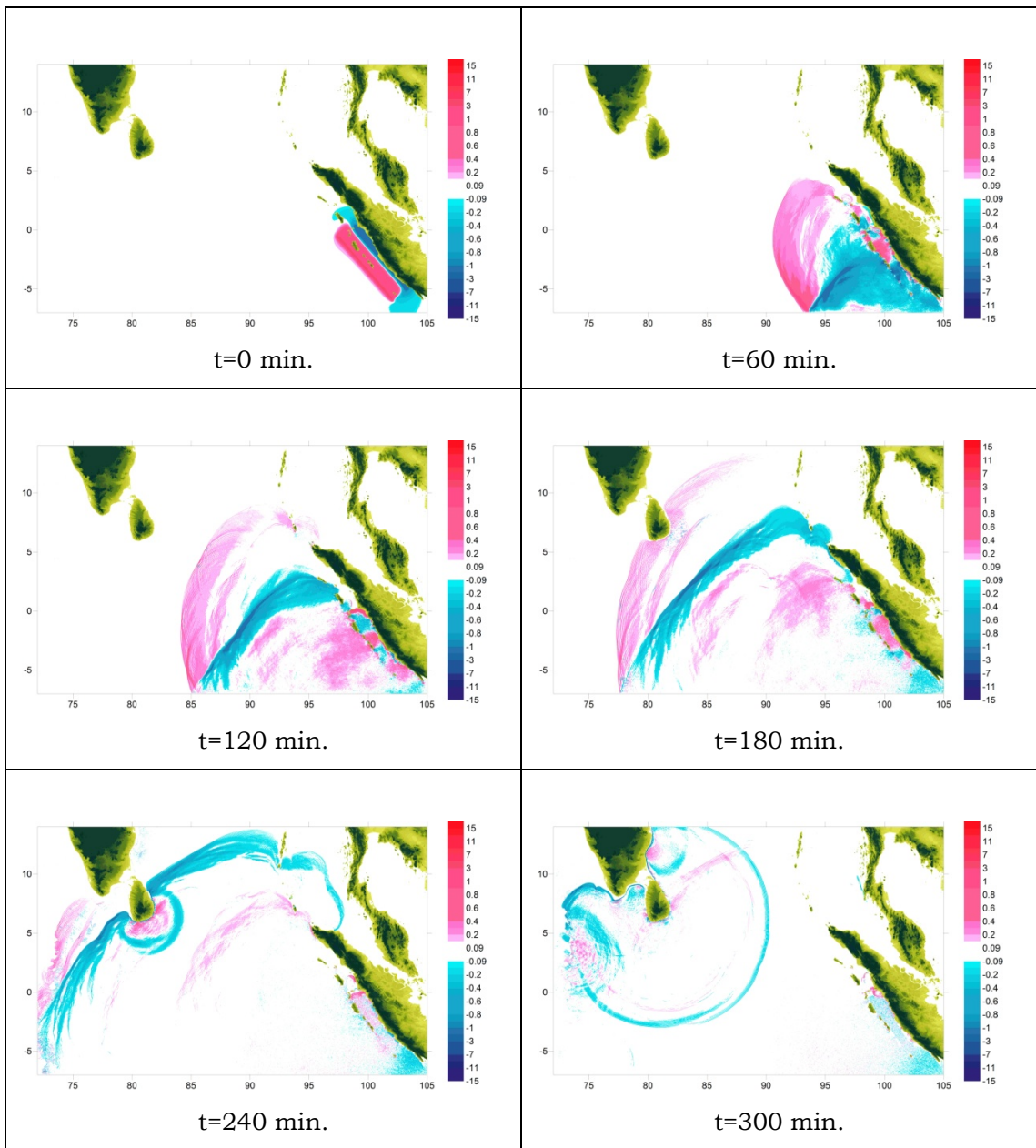


Figure 20. Sea states between $t=0$ and $t=300$ min for the 2nd case (McCloskey et al., 2007)

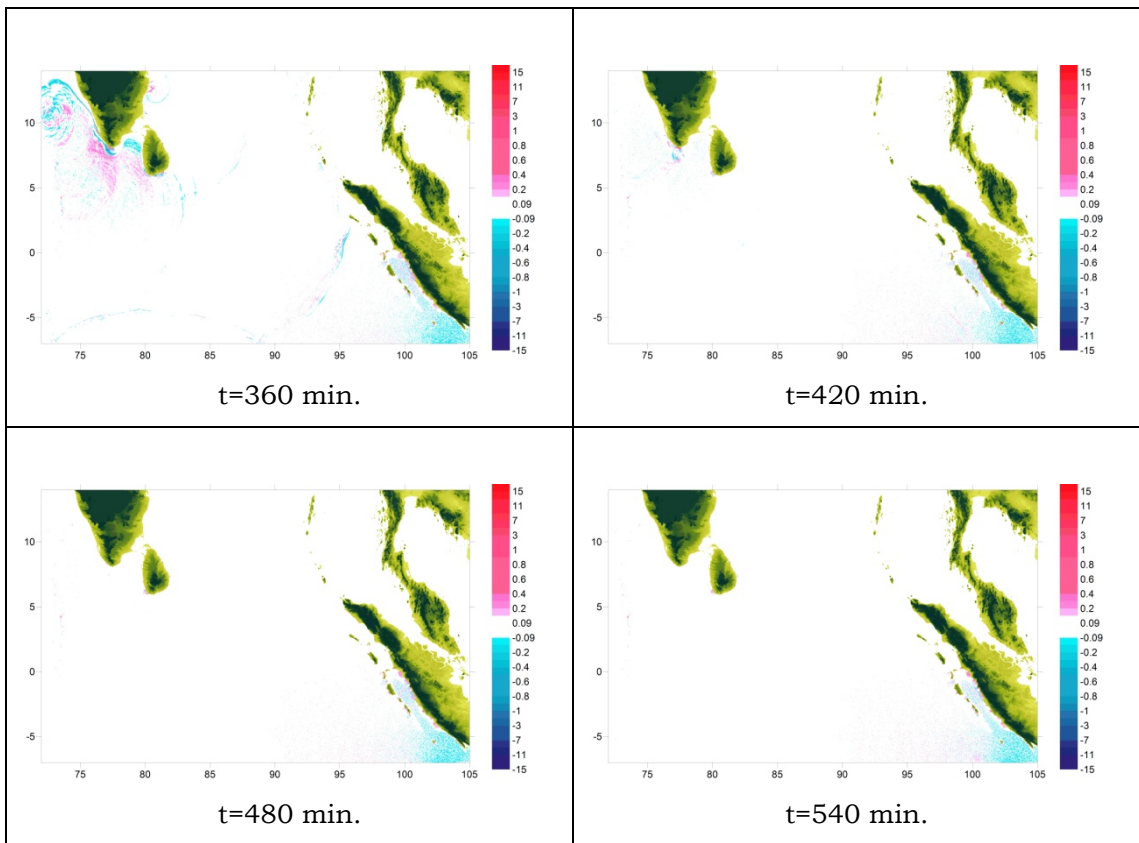


Figure 21. Sea states between $t=360$ and $t=540$ min. for the 2nd case (McCloskey et al., 2007)

The maximum positive and negative wave amplitudes in Domains C and E are computed and plotted in Figure 22 and 23. Also, the simulation results are tabulated and given in Table 10 and 11.

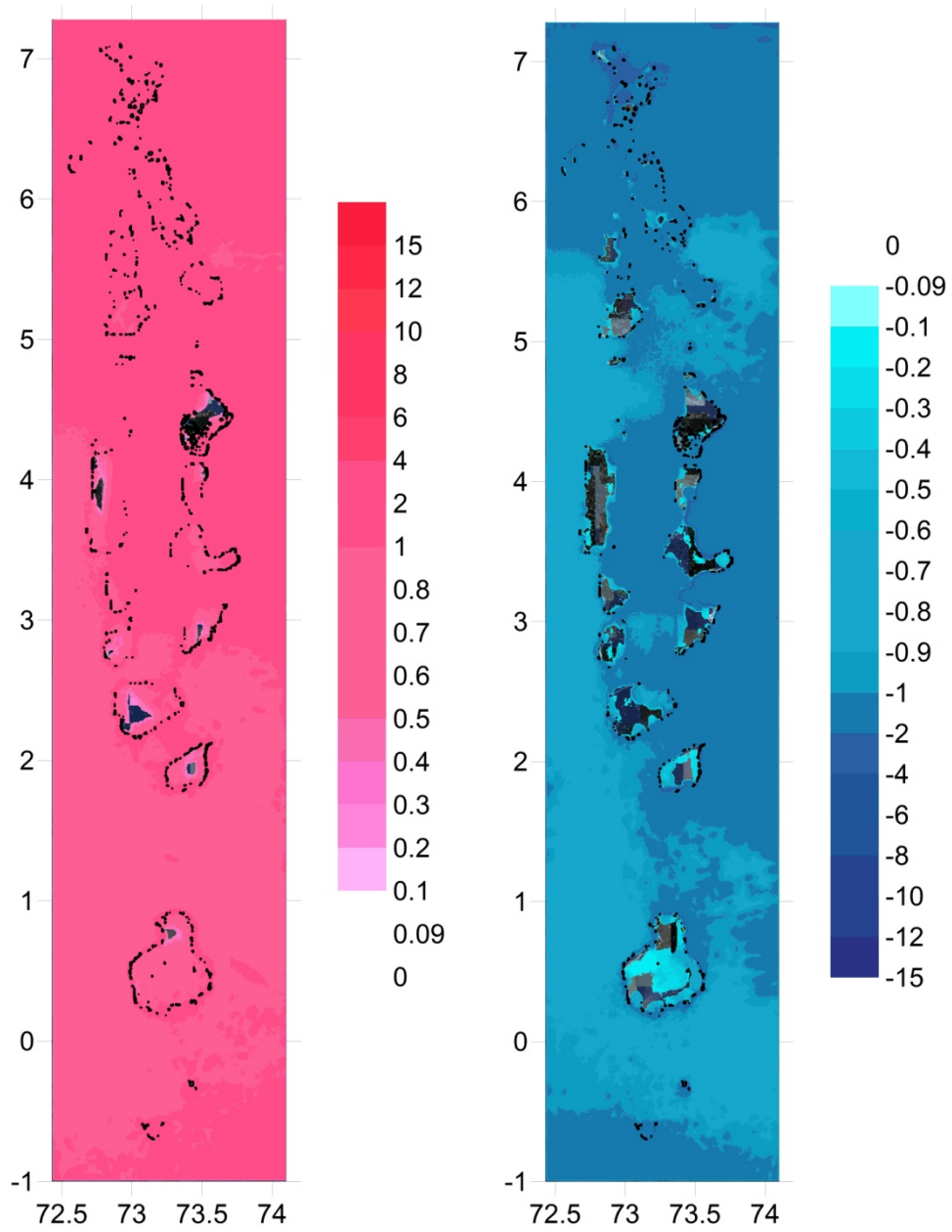


Figure 22. Maximum positive and negative wave amplitudes in Domain C for the 2nd case. (McCloskey et al., 2007)

Table 10. Results of simulation study in Domain C for the 2nd case. (McCloskey et al., 2007)

Name Of Gauge	Depth Of Gauge (m)	X Coord	Y Coord	Arrival Time Of First Wave (min)	Arrival Time Of Max. Wave (min)	Maximum (+) Wave Amp.(m)	Maximum (-) Wave Amp.(m)
Shaviyani	8.9	73.15	6.31667	240	294	1.6	-2.6
Olivefushi	15.6	73.6056	5.29447	232	319	1.6	-1.4
Donveli	2.3	73.55	4.25	228	280	2.0	-2.3
Kandooma	4.1	73.45	3.88333	229	318	1.6	-1.8
Vevaru	5.6	73.6056	2.96875	224	225	1.9	-1.8
Thaa	9.0	73.35	2.38333	223	229	1.8	-1.9
Laamu	14.6	73.5412	1.9119	220	234	3.3	-4.7
Fuvammulah	5.6	73.251	0.216667	216	219	1.7	-1.7
Hulhudu	8.3	73.2167	-0.583333	216	225	1.9	-1.7
Gan	8.9	73.45	-0.316667	214	257	2.3	-3.2
Hulhumeedho	18.3	73.2167	-0.633333	215	286	2.9	-2.5
Guradu	1.5	73.5853	5.43333	238	321	1.4	-0.8
Difuri	1.1	73.352	5.43333	238	321	1.6	-1.1
Muli	2.3	73.5896	2.93269	225	226	1.5	-0.5
Mavaru	1.1	73.552	0.4	218	294	1.0	0.0

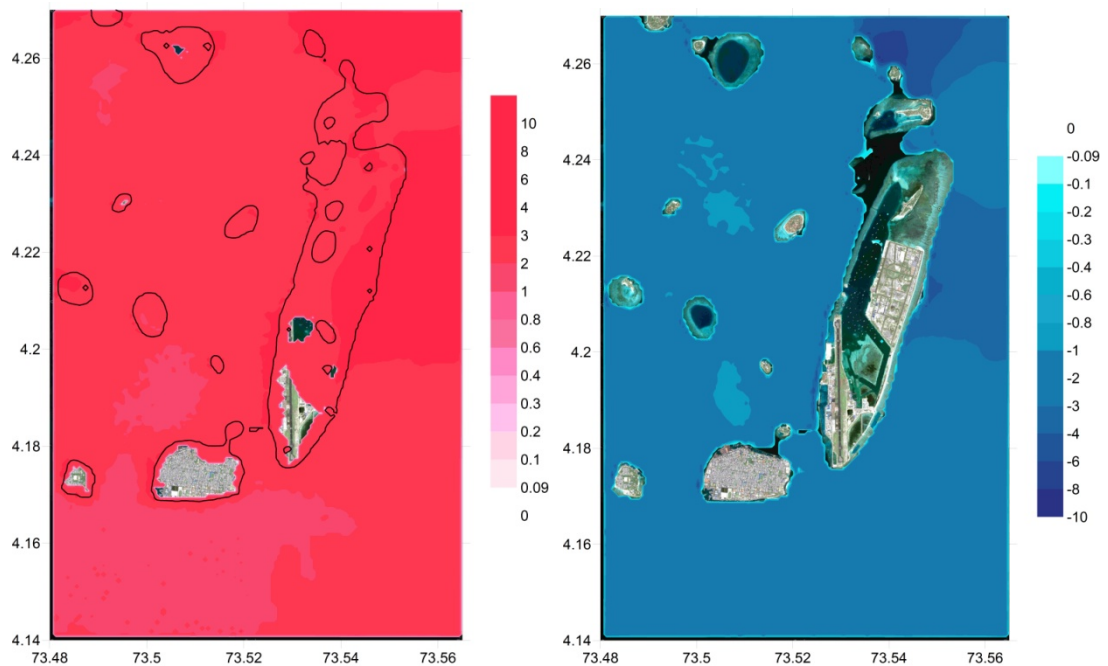


Figure 23. Maximum positive and negative wave amplitudes in Domain E for the 2nd case. (McCloskey et al., 2007)

Table 11. Results of simulation study in Domain E for the 2nd case. (McCloskey et al., 2007)

Name Of Gauge	Depth Of Gauge (m)	X Coord	Y Coord	Arrival Time of First Wave (min)	Arrival Time of Max. Wave (min)	Maximum (+)Wave Amp.(m)	Maximum (-)Wave Amp.(m)
A1	6.2	73.5367	4.25213	228	274	2.3	-2.0
B1	5.8	73.5287	4.21147	228	271	2.7	-1.8
C1	7.5	73.525	4.18066	227	274	2.2	-1.3
D1	4.9	73.5342	4.18	227	265	2.5	-1.6
E1	8.1	73.5416	4.19545	227	270	2.9	-2.5
F1	8.3	73.5441	4.2053	227	282	4.1	-3.4
G1	9.3	73.549	4.21578	227	270	4.5	-4.0
H1	4.6	73.5508	4.2281	227	270	4.1	-3.7
I1	7.7	73.5539	4.23919	227	270	3.5	-2.6
J1	8.1	73.5219	4.17389	227	274	2.1	-1.5
K1	7.1	73.5219	4.18313	227	274	2.2	-1.4
L1	5.3	73.5053	4.1819	227	271	2.3	-1.5
M1	7.9	73.5016	4.17512	227	277	4.7	-2.3
N1	8.3	73.5133	4.16896	227	275	2.1	-1.4

The maximum positive and negative wave amplitudes in Domain E are found to be 4.5 m. and -4.0 m. respectively.

4.2.3. Megathrust under the Batu and Mentawai Islands (Okal and Synolakis., 2007)

As the final case, which is significantly probable according to Okal and Synolakis (2007), was simulated to illustrate the effects of the far-field tsunami hazard in the Indian Ocean basin. The maximum positive and negative wave amplitudes observed in the simulation studies are plotted in Figure 24 and 25 for Domains C and E. Also, the simulation results are tabulated and given in Table 12 and 13.

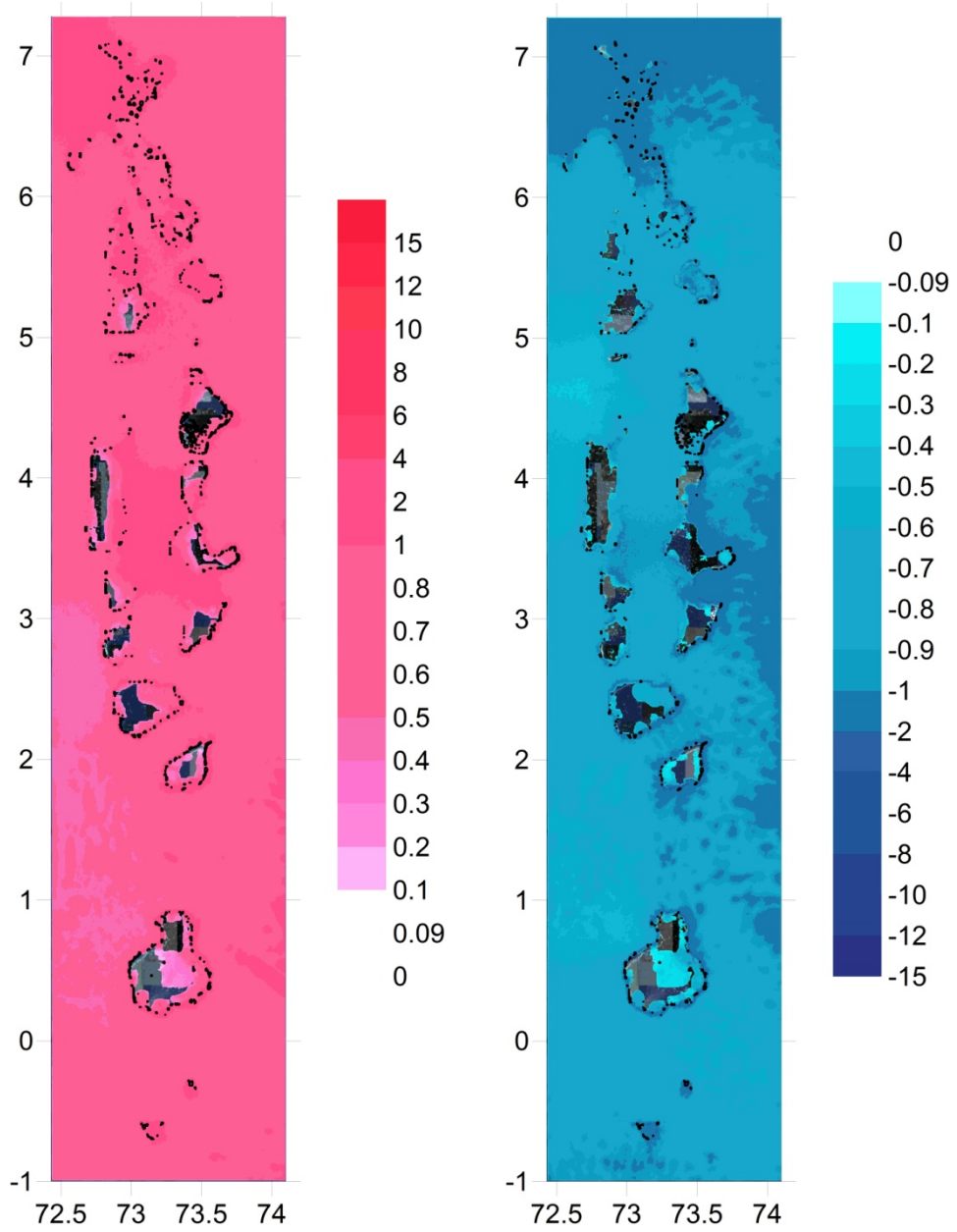


Figure 24. Maximum positive and negative wave amplitudes in Domain C for the 3rd case. (Okal and Synolakis, 2007)

Table 12. Results of simulation study in Domain C for the 3rd case. (Okal and Synolakis, 2007)

Name Of Gauge	Depth Of Gauge (m)	X Coord	Y Coord	Arrival Time Of First Wave (min)	Arrival Time Of Max. Wave (min)	Maximum (+) Wave Amp.(m)	Maximum (-) Wave Amp.(m)
Shaviyani	8.9	73.15	6.31667	245	293	1.6	-1.7
Olivefushi	15.6	73.6056	5.29447	236	322	1.5	-1.2
Donveli	2.3	73.55	4.25	232	265	2.1	-2.2
Kandooma	4.1	73.45	3.88333	233	285	1.0	-1.3
Vevaru	5.6	73.6056	2.96875	228	237	1.4	-1.5
Thaa	9.0	73.35	2.38333	226	276	1.5	-2.3
Laamu	14.6	73.5412	1.9119	223	257	3.3	-4.4
Fuvammulah	5.6	73.251	0.216667	219	230	1.5	-1.5
Hulhudu	8.3	73.2167	-0.583333	219	226	1.5	-1.4
Gan	8.9	73.45	-0.316667	217	292	1.8	-2.0
Hulhumeedho	18.3	73.2167	-0.633333	218	269	2.6	-2.4
Guradu	1.5	73.5853	5.43333	243	318	1.0	-0.6
Difuri	1.1	73.352	5.43333	243	317	1.0	-0.8
Muli	2.3	73.5896	2.93269	228	236	0.9	0.0
Mavaru	1.1	73.552	0.4	222	229	0.9	0.0

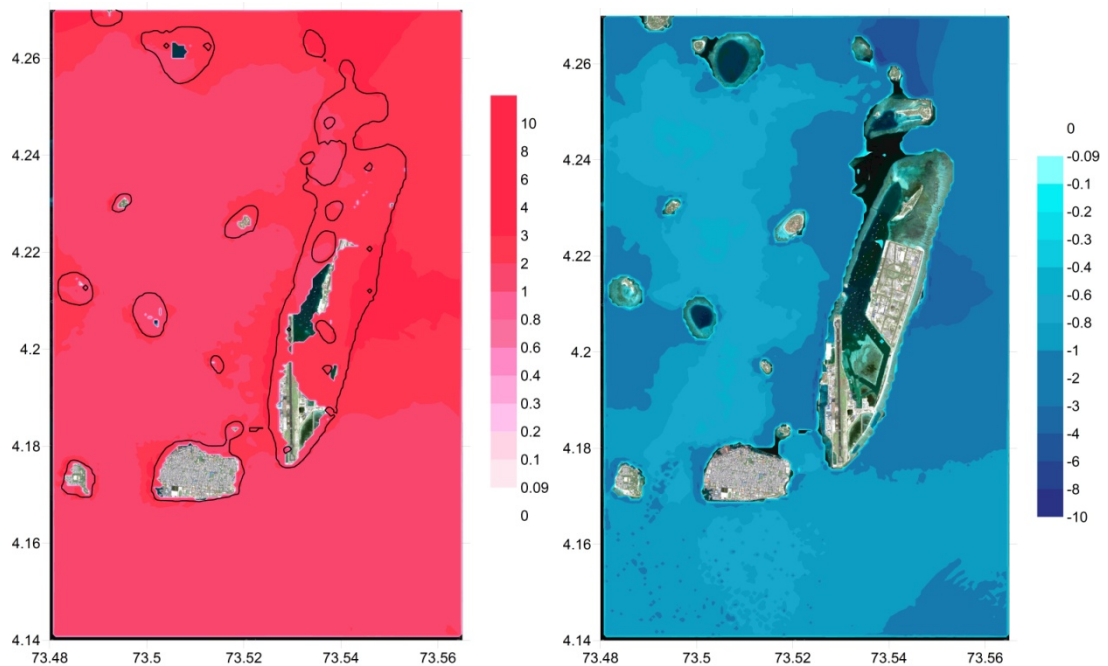


Figure 25. Maximum positive and negative wave amplitudes in Domain E for the 3rd case. (Okal and Synolakis, 2007)

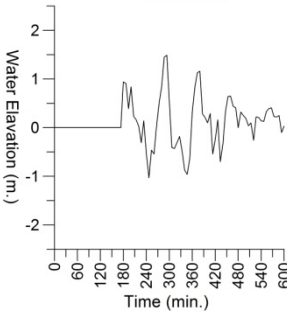
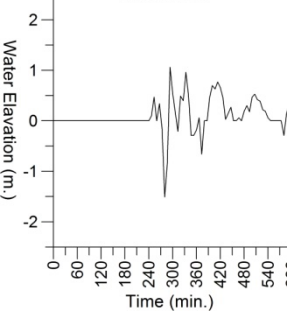
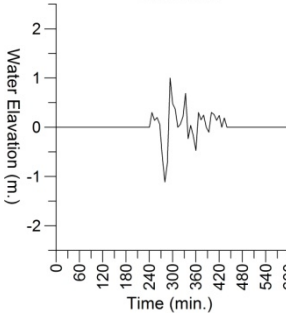
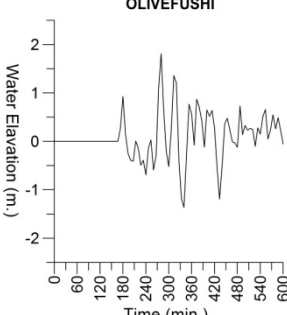
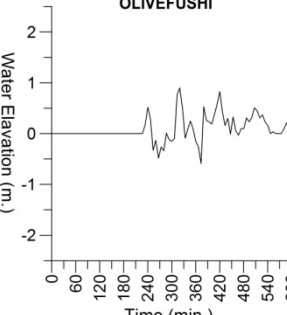
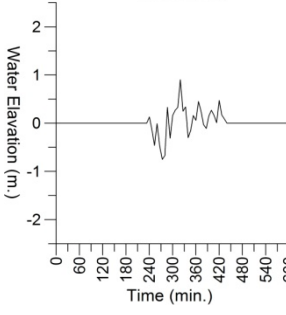
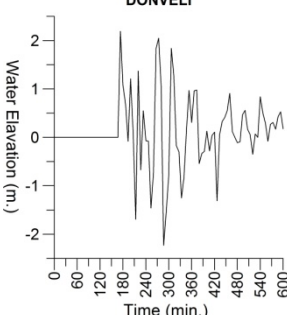
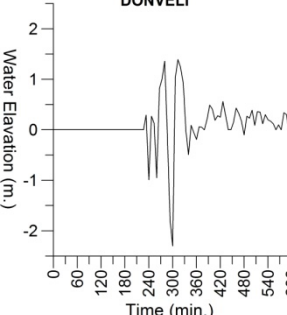
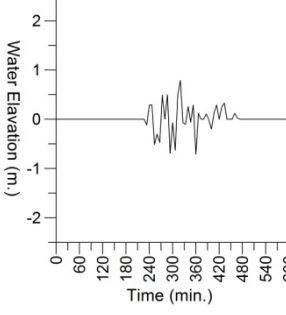
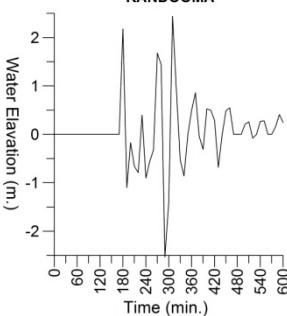
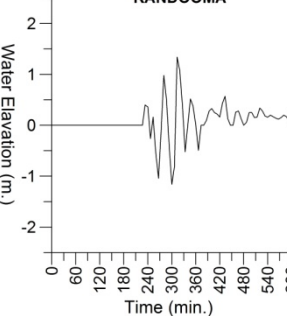
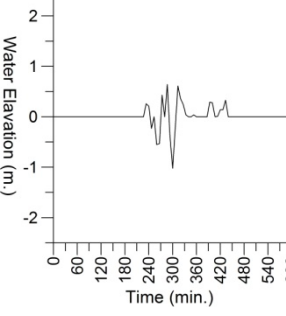
Table 13. Results of simulation study in Domain E for the 3rd case. (Okal and Synolakis, 2007)

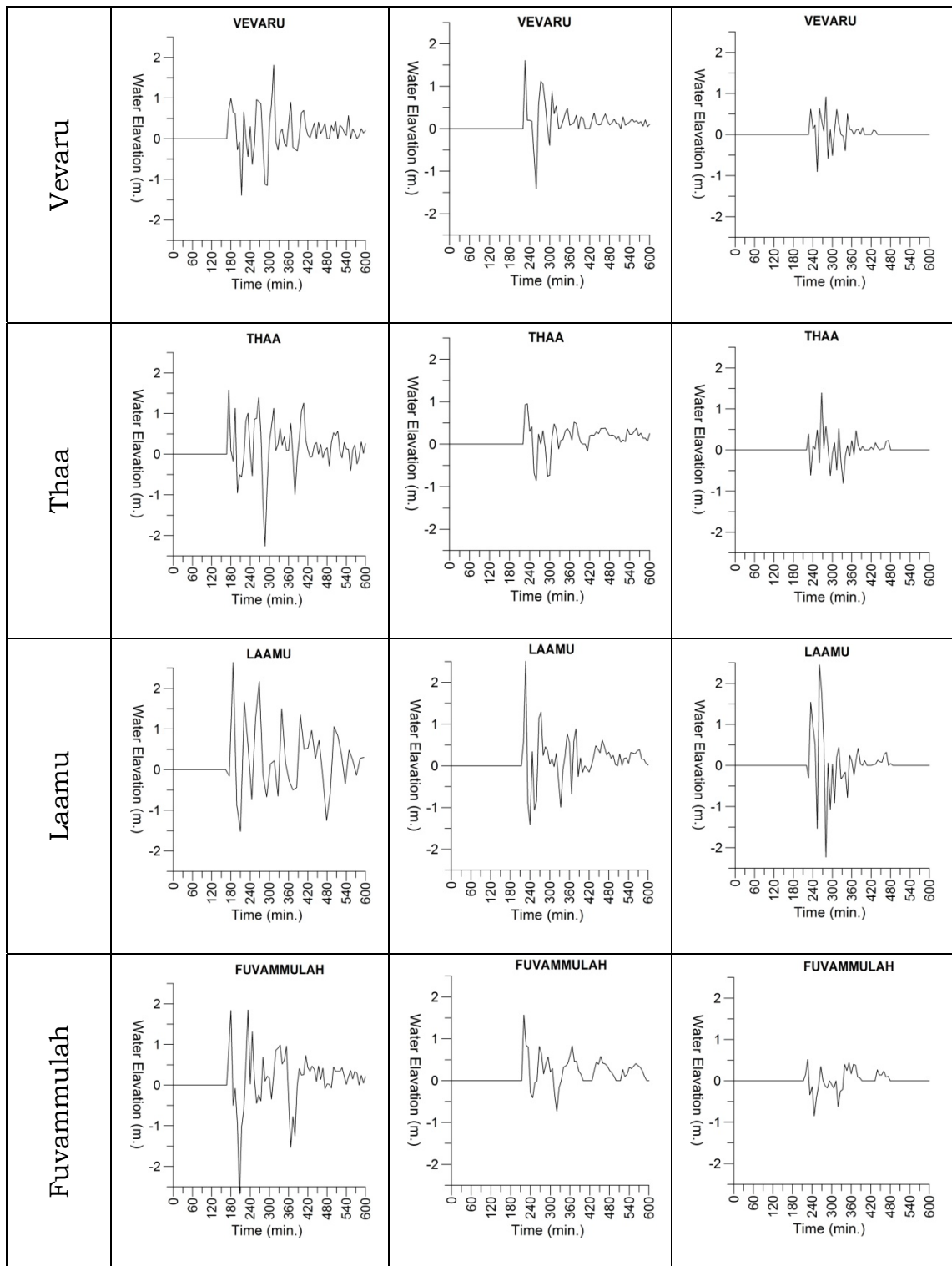
Name Of Gauge	Depth Of Gauge (m)	X Coord	Y Coord	Arrival Time of First Wave (min)	Arrival Time of Max. Wave (min)	Maximum (+)Wave Amp.(m)	Maximum (-)Wave Amp.(m)
A1	6.2	73.5367	4.25213	231	344	2.2	-1.6
B1	5.8	73.5287	4.21147	232	570	2.8	-3.3
C1	7.5	73.525	4.18066	231	273	2.1	-1.0
D1	4.9	73.5342	4.18	231	344	2.1	-1.1
E1	8.1	73.5416	4.19545	231	343	2.9	-2.1
F1	8.3	73.5441	4.2053	231	268	3.4	-3.1
G1	9.3	73.549	4.21578	231	268	3.4	-3.9
H1	4.6	73.5508	4.2281	231	305	3.1	-3.1
I1	7.7	73.5539	4.23919	231	264	2.5	-2.2
J1	8.1	73.5219	4.17389	231	272	1.8	-1.1
K1	7.1	73.5219	4.18313	231	273	2.0	-1.0
L1	5.3	73.5053	4.1819	231	306	1.9	-1.0
M1	7.9	73.5016	4.17512	231	307	4.0	-2.1
N1	8.3	73.5133	4.16896	231	273	1.8	-0.9

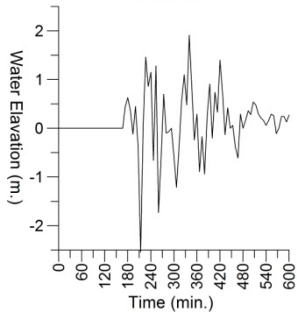
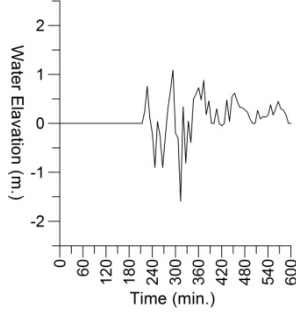
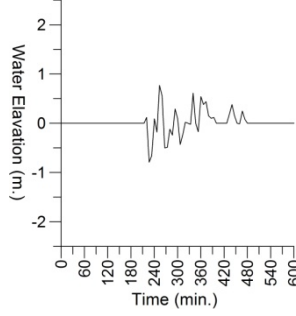
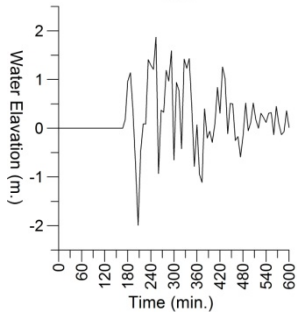
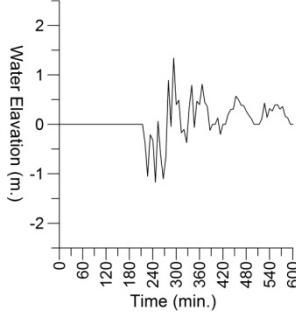
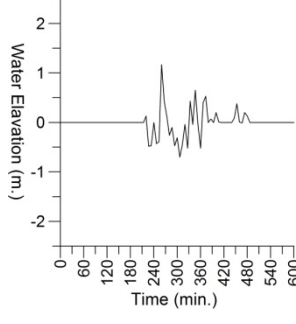
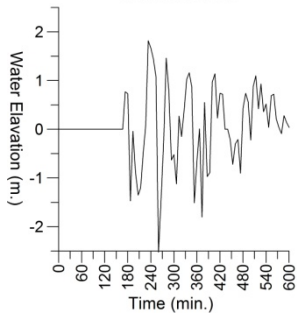
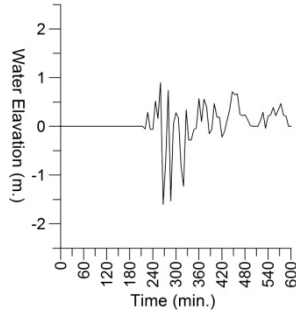
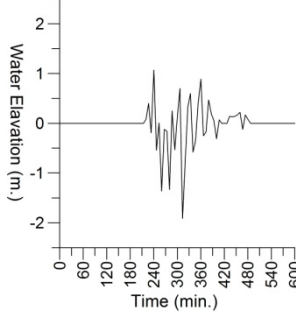
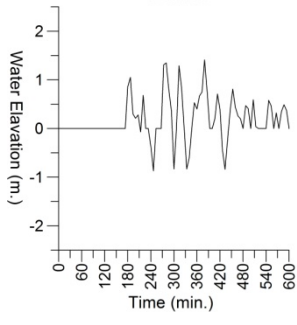
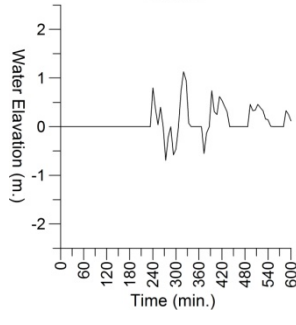
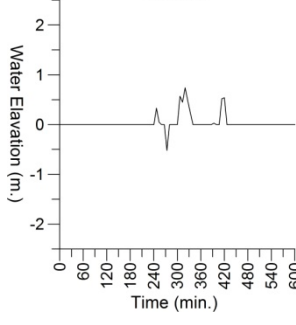
The maximum positive and negative wave amplitudes in Domain E are found to be 4.0 m. and -3.9 m. respectively.

4.3. Summary

After performing simulations of all three cases, the water surface fluctuations, computed in three simulations, are plotted in Figure 26 and Figure 27 for comparison. Moreover, the maximum positive and negative wave amplitudes are also tabulated in Table 14 and 15.

Name Of Gauge	1 st Case, Sumatra-Andaman Earthquake, 2004	2 nd Case, by McCloskey et al., 2007	3 th Case, by Okal and Synolakis, 2007
Shaviyani	<p style="text-align: center;">SHAVIYANI</p> 	<p style="text-align: center;">SHAVIYANI</p> 	<p style="text-align: center;">SHAVIYANI</p> 
Olivefushi	<p style="text-align: center;">OLIVEFUSHI</p> 	<p style="text-align: center;">OLIVEFUSHI</p> 	<p style="text-align: center;">OLIVEFUSHI</p> 
Donveli	<p style="text-align: center;">DONVELI</p> 	<p style="text-align: center;">DONVELI</p> 	<p style="text-align: center;">DONVELI</p> 
Kandooma	<p style="text-align: center;">KANDOOMA</p> 	<p style="text-align: center;">KANDOOMA</p> 	<p style="text-align: center;">KANDOOMA</p> 



Hulhudu	<p style="text-align: center;">HULHUDU</p> 	<p style="text-align: center;">HULHUDU</p> 	<p style="text-align: center;">HULHUDU</p> 
Gan	<p style="text-align: center;">GAN</p> 	<p style="text-align: center;">GAN</p> 	<p style="text-align: center;">GAN</p> 
Hulhumeedho	<p style="text-align: center;">HULHUMEEDHO</p> 	<p style="text-align: center;">HULHUMEEDHO</p> 	<p style="text-align: center;">HULHUMEEDHO</p> 
Guradu	<p style="text-align: center;">GURADU</p> 	<p style="text-align: center;">GURADU</p> 	<p style="text-align: center;">GURADU</p> 

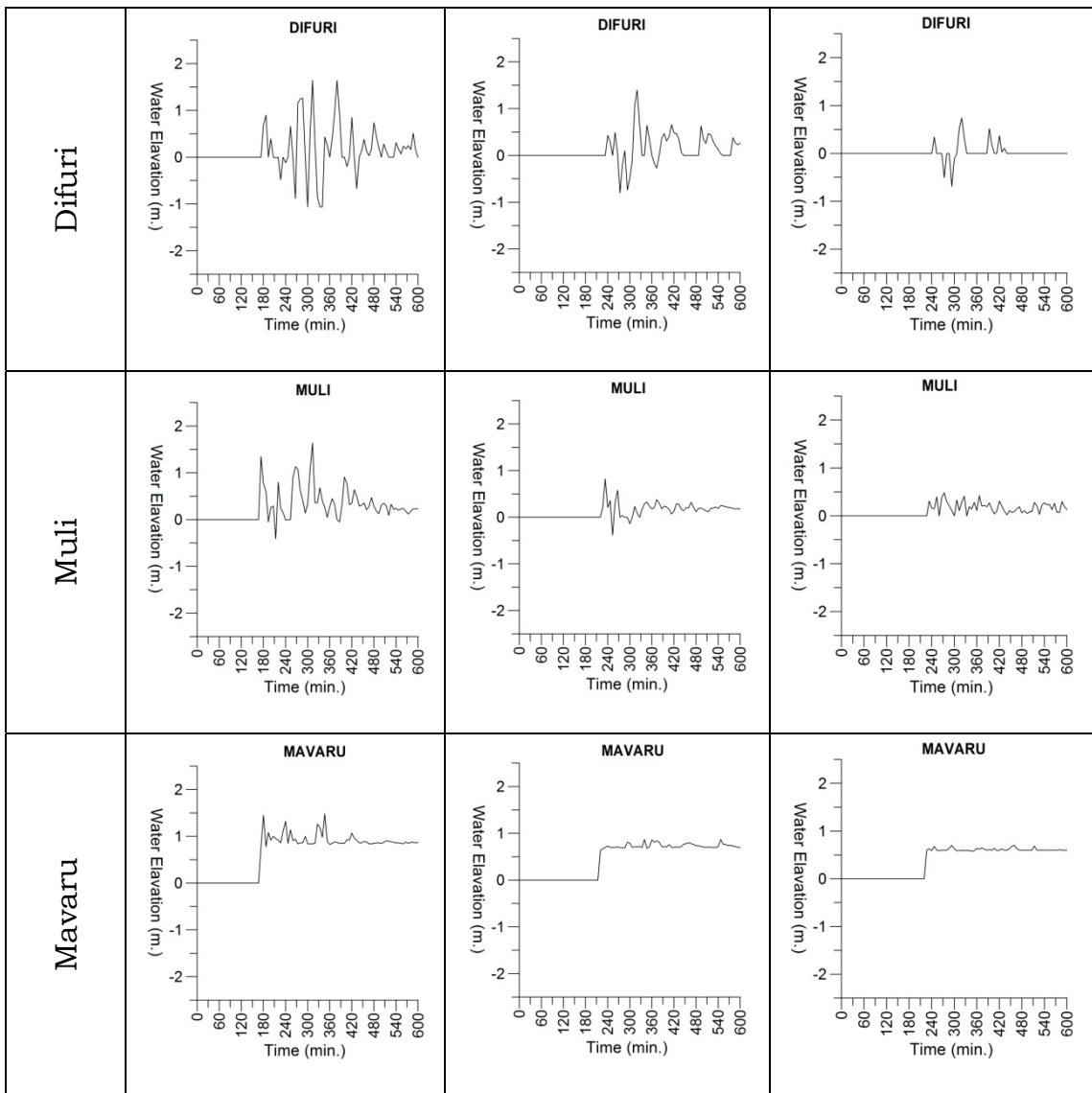
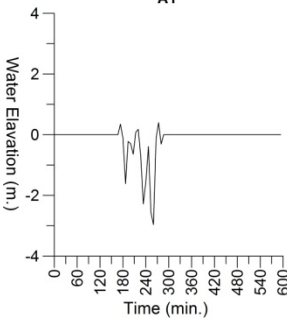
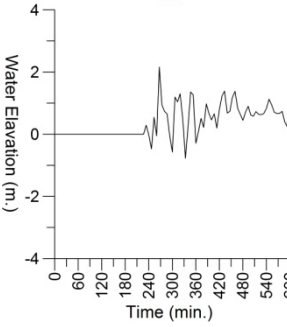
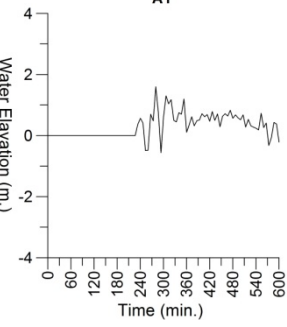
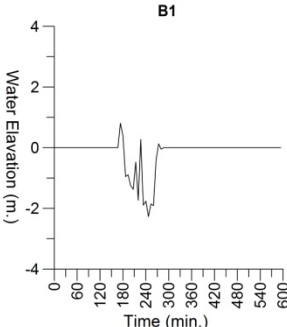
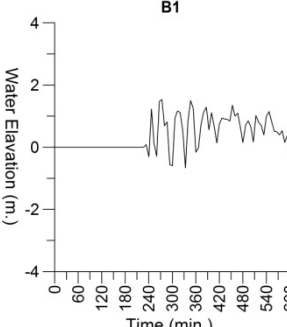
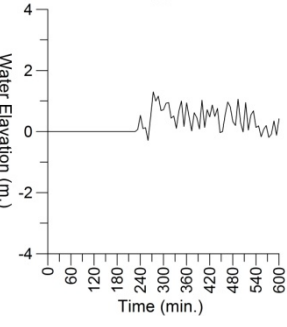
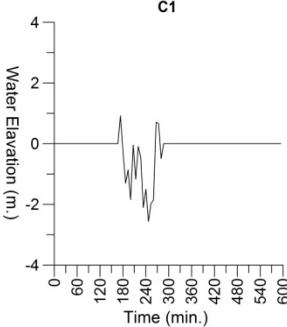
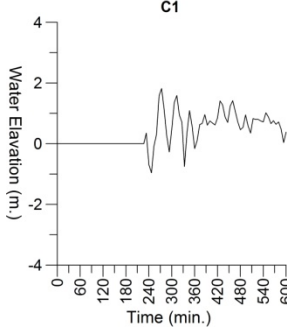
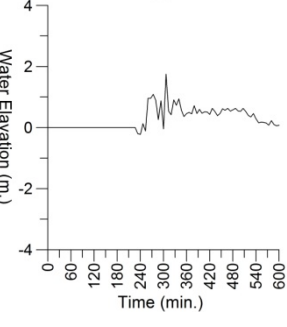
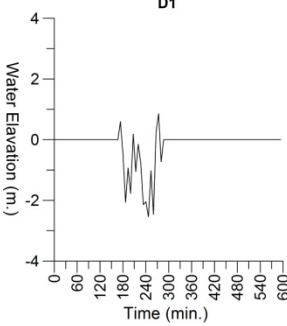
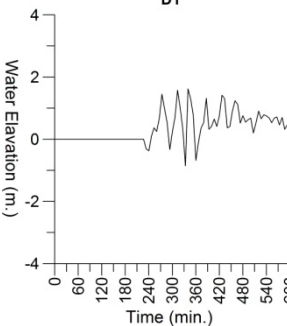
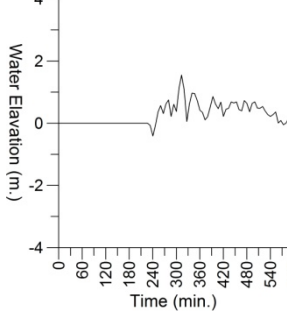
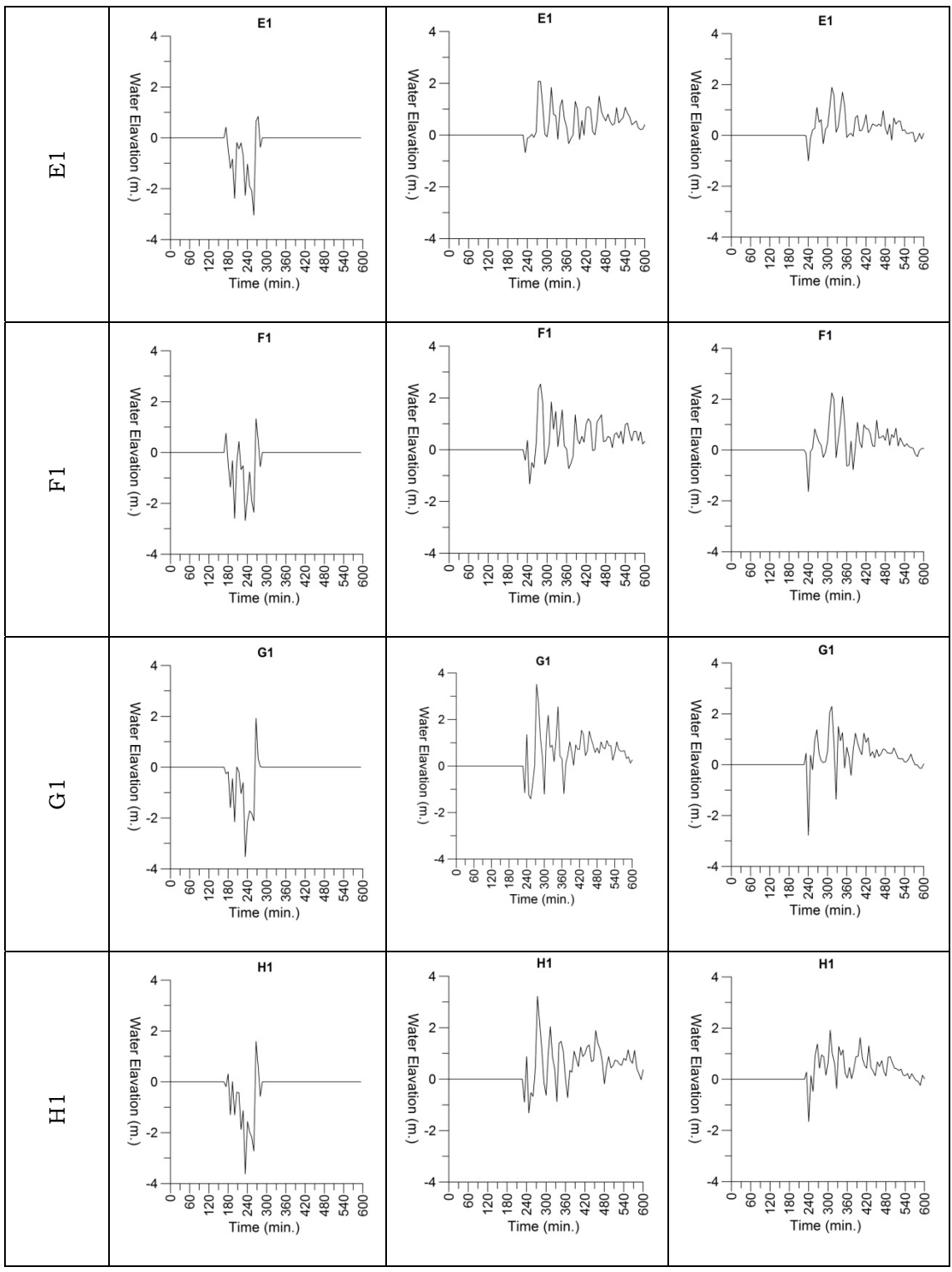
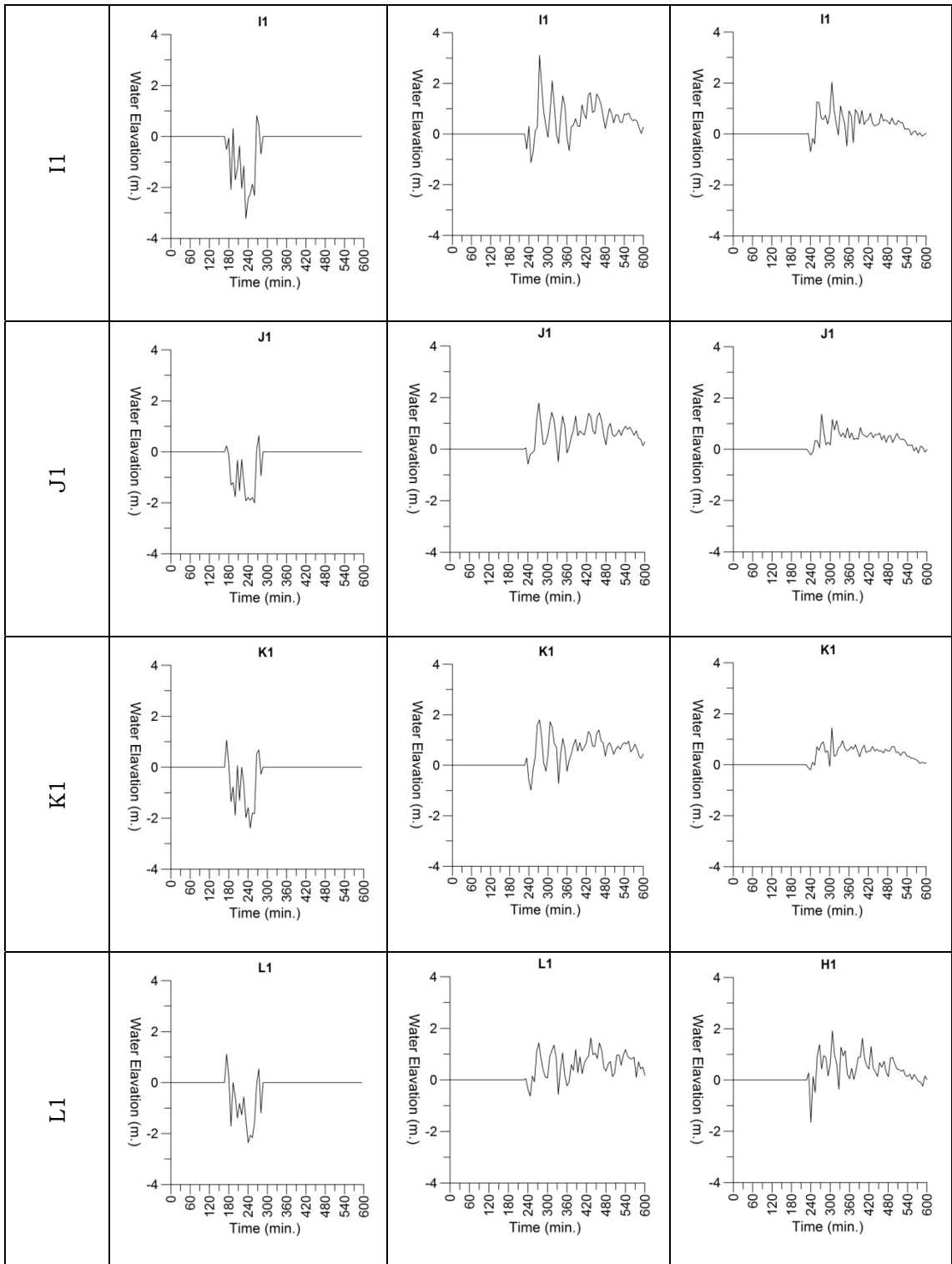


Figure 26. Time history of water surface fluctuations for selected gauges in Domain

C.

Name Of Gauge	1 st Case, Sumatra-Andaman Earthquake, 2004	2 nd Case, by McCloskey et al., 2007	3 th Case, by Okal and Synolakis, 2007
A1	<p style="text-align: center;">A1</p> 	<p style="text-align: center;">A1</p> 	<p style="text-align: center;">A1</p> 
B1	<p style="text-align: center;">B1</p> 	<p style="text-align: center;">B1</p> 	<p style="text-align: center;">B1</p> 
C1	<p style="text-align: center;">C1</p> 	<p style="text-align: center;">C1</p> 	<p style="text-align: center;">C1</p> 
D1	<p style="text-align: center;">D1</p> 	<p style="text-align: center;">D1</p> 	<p style="text-align: center;">D1</p> 





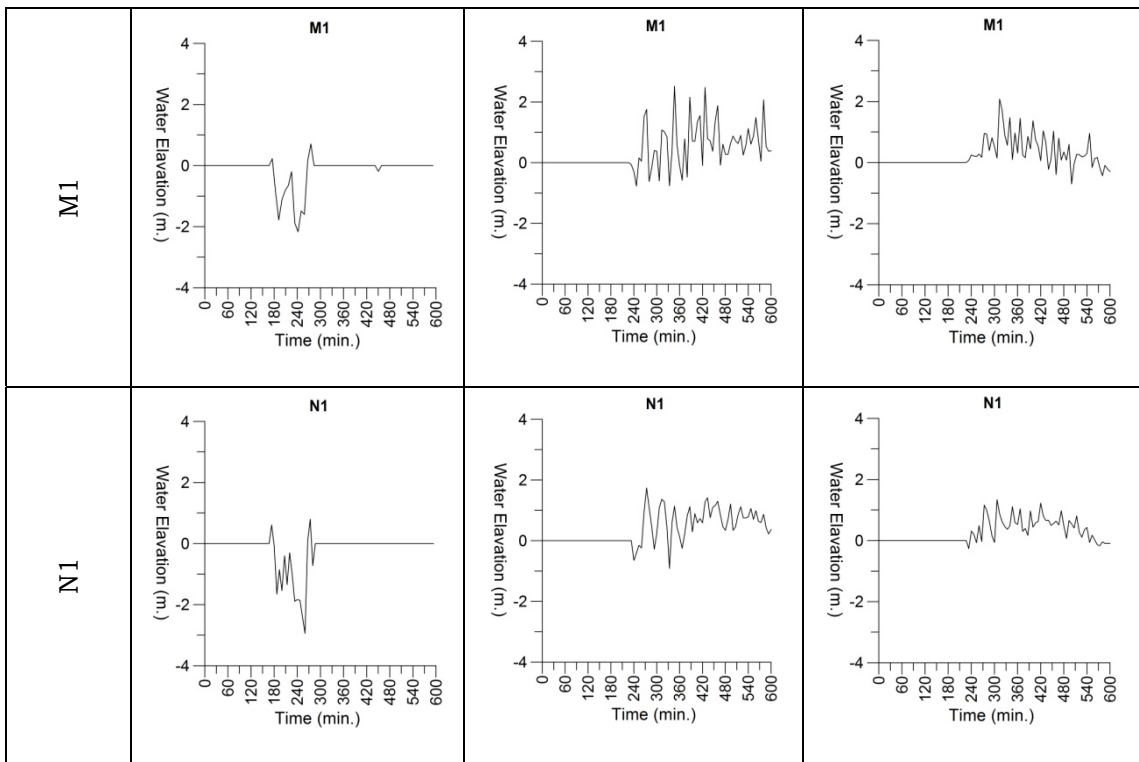


Figure 27. Time history of water surface fluctuations for selected gauges in Domain E.

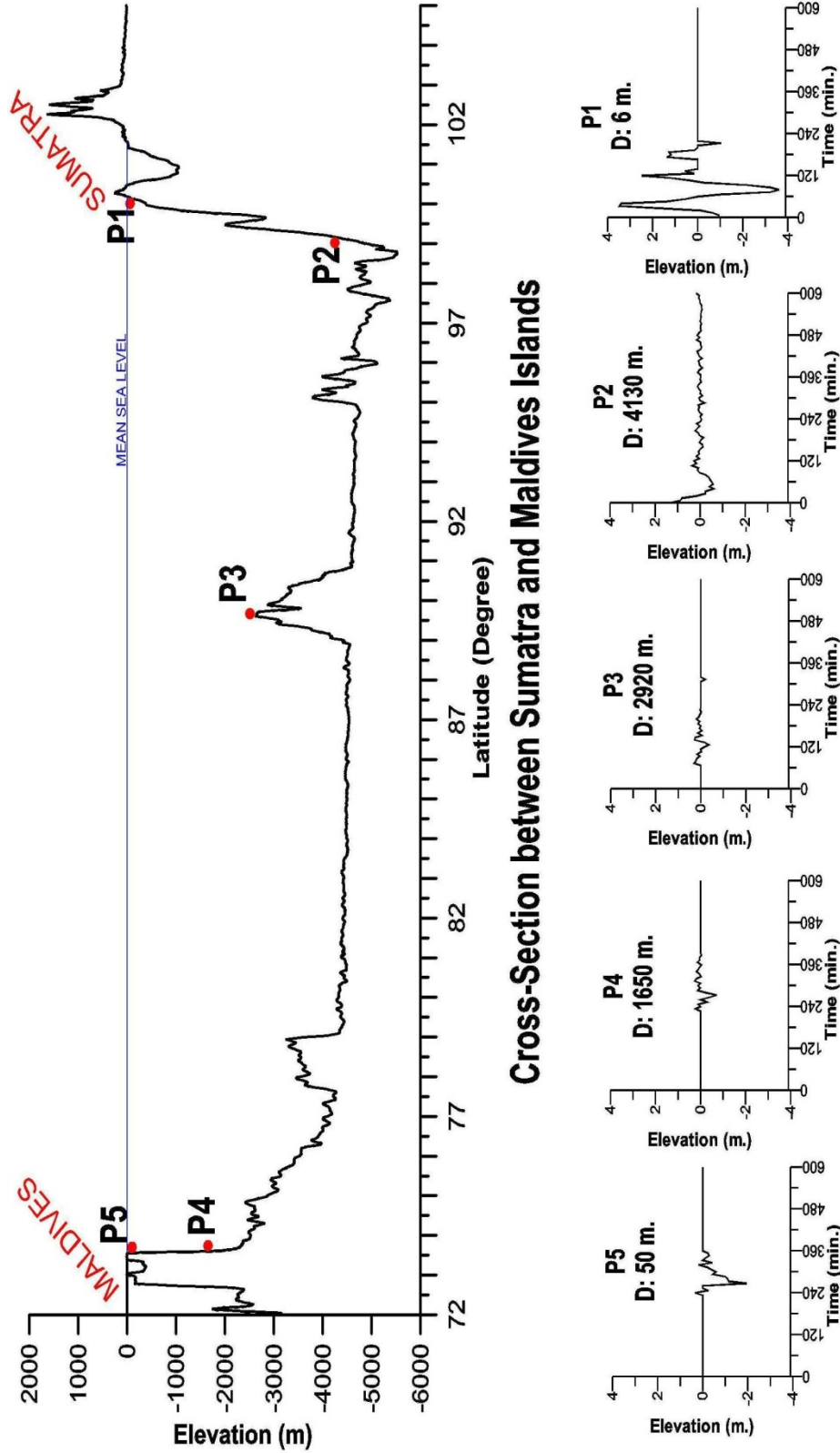
Table 14. Summary of simulation studies for all cases in Domain C.

Name Of Gauge	1 st Case, Sumatra-Andaman Earthquake, 2004		2 nd Case, by McCloskey et al., 2007		3 th Case, by Okal and Synolakis, 2007	
	Maximum (+) Wave Amp.(m)	Maximum (-) Wave Amp.(m)	Maximum (+) Wave Amp.(m)	Maximum (-) Wave Amp.(m)	Maximum (+) Wave Amp.(m)	Maximum (-) Wave Amp.(m)
Shaviyani	2.0	-0.4	1.6	-2.6	1.6	-1.7
Olivefushi	2.2	-1.4	1.6	-1.4	1.5	-1.2
Donveli	3.3	-2.3	2.0	-2.3	2.1	-2.2
Kandooma	2.5	-1.6	1.6	-1.8	1.0	-1.3
Vevaru	2.1	-1.3	1.9	-1.8	1.4	-1.5
Thaa	2.5	-1.5	1.8	-1.9	1.5	-2.3
Laamu	6.0	-3.4	3.3	-4.7	3.3	-4.4
Fuvammula	2.5	-1.8	1.7	-1.7	1.5	-1.5
Hulhudu	2.9	-1.5	1.9	-1.7	1.5	-1.4
Gan	2.8	-2.6	2.3	-3.2	1.8	-2.0
Hulhumeed.	3.1	-2.3	2.9	-2.5	2.6	-2.4
Guradu	1.8	0.0	1.4	-0.8	1.0	-0.6
Difuri	2.0	0.0	1.6	-1.1	1.0	-0.8
Muli	1.9	-0.3	1.5	-0.5	0.9	0.0
Mavaru	1.9	0.0	1.0	0.0	0.9	0.0

When the time history of water surface fluctuations computed were compared, simulation based on McCloskey et al, 2007 shows higher wave amplitudes in the islands focused on this study. In addition to this, for a better understanding of the transoceanic propagation of tsunamis in Indian Ocean, cross-sectional profile between Sumatra and Maldives Islands was plotted and at some points time history of water level fluctuations are illustrated in Figure 28 for this scenario.

Table 15. Summary of simulation studies for all cases in Domain E.

Name Of Gauge	1 st Case, Sumatra-Andaman Earthquake, 2004		2 nd Case, by McCloskey et al., 2007		3 th Case, by Okal and Synolakis, 2007	
	Maximum (+) Wave Amp.(m)	Maximum (-) Wave Amp.(m)	Maximum (+) Wave Amp.(m)	Maximum (-) Wave Amp.(m)	Maximum (+) Wave Amp.(m)	Maximum (-) Wave Amp.(m)
A1	1.9	-0.6	2.3	-2.0	2.2	-1.6
B1	2.4	-0.7	2.7	-1.8	2.8	-3.3
C1	1.3	-0.6	2.2	-1.3	2.1	-1.0
D1	1.3	-0.5	2.5	-1.6	2.1	-1.1
E1	1.8	-1.1	2.9	-2.5	2.9	-2.1
F1	2.2	-1.4	4.1	-3.4	3.4	-3.1
G1	2.9	-2.1	4.5	-4.0	3.4	-3.9
H1	2.8	-1.6	4.1	-3.7	3.1	-3.1
I1	2.9	-1.5	3.5	-2.6	2.5	-2.2
J1	1.1	-0.4	2.1	-1.5	1.8	-1.1
K1	1.3	-0.6	2.2	-1.4	2.0	-1.0
L1	1.5	-0.4	2.3	-1.5	1.9	-1.0
M1	1.2	-0.4	4.7	-2.3	4.0	-2.1
N1	1.3	-0.5	2.1	-1.4	1.8	-0.9
A2 (at land)	2.4	0.0	2.6	0.0	2.3	0.0
B2 (at land)	1.0	0.0	2.3	0.0	2.1	0.0
C2 (at land)	1.7	0.0	3.1	0.0	2.7	0.0
D2 (at land)	2.4	0.0	3.9	0.0	3.4	0.0
E2 (at land)	1.4	0.0	2.4	0.0	2.1	0.0
F2 (at land)	1.3	0.0	2.2	0.0	2.3	0.0
G2 (at land)	1.6	0.0	2.3	0.0	2.1	0.0
H2 (at land)	2.0	0.0	2.3	0.0	1.9	0.0



Cross-Section between Sumatra and Maldives Islands

Time Histories for Selected Points

Figure 28. Cross-Section of the line between Sumatra and Maldives Islands and time history graphs of water level fluctuations at some points.

CHAPTER V

DISCUSSION AND CONCLUSION

5.1. General Evaluation

The rupture characteristics of tsunami triggering earthquakes cannot be accurately estimated by using only available seismic data. In order to perform tsunami modeling, the rupture characteristics of different scenarios should be defined and used as an input parameter together with the fine bathymetric data.

Fine gridded bathymetric data is another significant input parameter for numerical tsunami-modeling. GEBCO Grid Viewing and data access software was used together with Google Earth software to obtain the bathymetric data of study domain. Some correlation studies in the project area were carried out in order to minimize the variations between planer and spherical projection of the earth in GEBCO and Google Earth.

After performing simulation studies, the characteristics of far-field tsunamis are given and illustrated in respective part of the thesis.

As the first case, Sumatra-Andaman earthquake, 2004, was modeled to verify the validity of the modeling studies. The rupture parameters of this earthquake were defined by Earth Sciences Department and Institute of Geophysics and Planetary Physics of University of

California (Lay et al., 2005). According to these input parameters, simulation study was done and results are given in Chapter 4.2.1. The evaluation of the modeling studies were done in the same chapter by comparing results with the site observations (Keating and Helsley, 2005) and tide gauge recordings of Sumatra – Andaman earthquake, 2004 (Merrifield et al.,2005).

The second case is the worst scenario defined by McCloskey et al., 2007. In that case, the rupture parameters given in Table 3, were used and corresponding results of simulation are given in chapter 4.2.2.

As the final case, another realistic and probable earthquake scenario in Indian Ocean was tried to find in the literatures. In that respect, Okal and Synolakis (2007) defined Scenario 2A, which takes into account the partial strain release in its northern segment during the 2007 Bengkulu event. Rupture parameters of Scenario 2A are given in Table 4 and result of this more probably event are shown in chapter 4.2.3.

5.2. Discussion and Conclusion

According to the simulation results, the arrival time of a tsunami which had been initiated at Sumatra zone of Sunda Arc is in between 225 and 232 minutes for Maldives and corresponding wave amplitudes at the gauge points are given in respective tables. It is obvious that effects of the far-field tsunami generated by an earthquake in Sumatra zone, is hazardous for Maldives which also experienced during December 26, 2004 Indian Ocean tsunami.

It should also be noted that due to the low-lying structural settlement in the Maldives, especially populated areas are still under the risk of inundation.

On the other hand, although, this study is focused mainly on Maldives islands considering far field effects of West Sumatra originated tsunamis, it should be indicated here that the near field effects of these tsunamis on the islands and towns located west of Sumatra will be much more destructive comparing to far field effects. The arrival time of these tsunamis to nearest coastal areas are very short which may not permit sufficient time for warning during tsunami.

As a final, it should also be noted that, there are still some uncertainties in the simulations which come from the uncertainty of the tsunami source parameters and accuracy of the bathymetry at shallow areas.

5.3. Suggestions for Further Studies

In this study, far-field propagation of tsunamis in Indian Ocean was investigated focusing on the Sumatra and Maldives Islands principally. For the worst case scenarios the tsunami modeling study case studies were applied to the specified locations, using rupture-specific tsunami sources which can generate tsunamis.

Since, the run up heights, found after simulation studies, are hazardous for Maldives, inundation zones should be determined and accordingly, evacuation plans and mitigation strategies should be developed because of the low-lying structures in Maldives.

It's also suggested that, in Indian Ocean, the effects of far-field tsunamis, propagated from an earthquake around Sumatra, should be studied deeply not only for Maldives but also for other populated areas, such as; Sri Lanka and India. In that case the negative effects of a far-field tsunami become more evident, since there are no steep coral atolls surroundings in that zone.

REFERENCES

Keating, B. and Helsley, C., 2004 Indian ocean tsunami on the maldives islands: initial observations, 2005.

Blewitt, G., Kreemer, C., Hammond, W.C., Plag, H.P., Stein, S. and Okal, E., Rapid determination of earthquake magnitude using GPS for tsunami warning systems, 2006.

Briggs, R.W., Sieh, K., Meltzner, A.J., Natawidjaja, D., Galetzka, J., Suwargadi, B., Hsu, Y., Simons, M., Hananto, N., Suprihanto, I., Prayudi, D., Avouac, J.P., Prawirodirdjo, L., Bock, Y., Deformation and slip along the Sunda megathrust in the great 2005 Nias–Simeulue earthquake, 2006.

California Institute of Technology, Another Large Earthquake Off Coast Of Sumatra Likely, 2008.

Chlieh, M., et al., Coseismic slip and afterslip of the Great (Mw9.15) Sumatra–Andaman Earthquake of 2004, 2007.

Geist, E., Bilek, S.L., Arcas, D., Titov, V.V., Differences in tsunami generation between the December 26, 2004 and March 28, 2005 Sumatra earthquakes, Earth Planets Space, 2005.

Goto, C. and Ogawa, Y., Numerical Method of Tsunami Simulation With the Leap-Frog Scheme, 1991.

Harbitz, C.B., Løvholt, F., Pedersen, G. & Masson, D.G., Mechanisms of tsunami generation by submarine landslides, *Norwegian Journal of Geology*, 2006.

Harinarayana, T., and Hirata, N., Destructive Earthquake and Disastrous Tsunami in the Indian Ocean, What next?, 2005.

Imamura F., Tsunami Numerical Simulation with the staggered leap-frog scheme (Numerical code of TUNAMI-N1), 1989.

Imamura, F., Yalciner, A.C., Ozyurt, G., Tsunami Modelling Manual, 2006.

International Tsunami Information Center (ITIC), 25 October 2010, Mw 7.7, Mentawai Region, Indonesia, 2010.

Lay, T., Kanamori, H., Ammon, C.J., Nettles, M., Ward, S.N., Aster, R.C., Beck, S.L., Bilek, S.L., Brudzinski, M.R., Butler, R., DeShon, H.R., The Great Sumatra-Andaman Earthquake of 26 December 2004, 2005.

Leblond, P., Mysak, L.A., *Waves in the Ocean*, Elsevier, 1978.

Megawati, K., and Pan, T.C., Regional Seismic Hazard Posed by the Mentawai Segment of the Sumatran Megathrust, 2009.

McCloskey, J., Nalbant, S.S., Steacy, S., Earthquake risk from co-seismic stress, 2005.

McCloskey, J., Antonioli, A., Piatanesi, A., Sieh, K., Steacy, S., Nalbant, S.S., Cocco, M., Giunchi, C., Huang, J.D., Dunlop, P.,

Tsunami threat in the Indian Ocean from a future megathrust earthquake west of Sumatra, 2007.

Merrifield, M.A., Firing, Y.L., Aarup, T., Agricole, W., Brundrit, G., Seng, C., Farre, R., Kilonsky, B., Knight, W., Kong, L., Magori, C., Manurung, P., McCreery, C., Mitchell, W., Pillay, S., Schindele, F., Shillington, F., Testut, L., Wijeratne, E.M.S., Caldwell, P., Jardin, J., Nakahara, S., Porter, Y., Turetsky, N, Tide gauge observations of the Indian Ocean tsunami, December 26, 2004, 2005.

Natawidjaja, D. H., Sieh, K., Ward, S., Cheng, H., Edwards, R.L., Galetzka, J., Suwargadi, B. W., Paleogeodetic records of seismic and aseismic subduction from central Sumatran Microatolls, 2004.

Natawidjaja, D. H., Sieh, K., Chlieh, M., Galetzka, J., Suwargadi, B. W., Cheng, H., Edwards, R.L., Avouac, J. P., Ward, S., The giant Sumatran megathrust ruptures of 1797 and 1833, 2006.

National Oceanic and Atmospheric Administration Center of Tsunami Research, <http://nctr.pmel.noaa.gov/indo20041226/tsunami1.pdf>, last visited on December 2010.

Okal, E.A., Synolakis, C., Far-field tsunami hazard from mega-thrust earthquakes in the Indian Ocean, 2007.

Okal, E.A., Synolakis, C., Source discriminants for near-field tsunamis, 2004.

Piatanesi, A., Lorito, S., Rupture process of the 2004 Sumatra–Andaman earthquake from tsunami waveform inversion, 2007.

UNEP-WCMC, Shoreline Protection and other Ecosystem Services from Mangroves and Coral Reefs, 2006.

Shuto, N., Goto, C., Imamura, F., Numerical simulation as a means of warning for near field tsunamis, 1990.

Subarya, C., Prawirodirdjo, L., Avouac, J.P., Bock, Y., Sieh, K., Meltzner, A.J., Natawidjaja, D.H., McCaffrey, R., Plate-boundary deformation associated with the great Sumatra–Andaman earthquake, 2006.

Synolakis, C. E, Liu, P. L. F., Yeh, H., Workshop on Long Wave Runup Models, 2004.

Sümer, B.M., Ansal, A., Çetin, K.O., Damgaard, J., Günbak, A.R., Ottesen Hansen, N-E, Sawicki, A., Synolakis, C.E., Yalçiner, A.C., Yüksel, Y., Zen, K., Earthquake-Induced Liquefaction around Marine Structures, J. of Waterway Port, Coastal and Ocean Engineering, ASCE, doi: 10.1061/(ASCE)0733-950X(2007)133:1(55), 2007.

Vigny, C., W. J. F. Simons, S. Abu et al., Insight into the 2004 Sumatra–Andaman earthquake from GPS measurements in Southeast Asia, 2005.

Ward, S.N., Landslide tsunami, Journal of Geophysical Research, 2001.

Yalçiner, A.C., Kuran, U, Imamura, F., Satioğlu, C., İnsel, I., Dilmen, D.I., Disposaptono, S., Shareef M., Propagation of Possible Tsunami from Seismic Gap at Western Sumatra and towards Western Indian Ocean, COMPASS Conference, 2008.

<http://yalciner.ce.metu.edu.tr/compass/Proceedings/> , last visited on December 2010.

Yalçiner, A. C., Synolakis, C. E, Gonzales, M., Kanođlu, U., Inundation Map and Test Sites of EU TRANSFER Project, 2007.

Yalçiner, A. C., Pelinovsky, E., Zaytsev, A., Kurkin, A., Özer, C., and Karakuş, H., NAMI DANCE Manual, 2006, <http://namidance.ce.metu.edu.tr> , last visited on December 2010.